

Hilde Nordvik

Digital Twin Modelling of High Voltage DC Generator

June 2019

NTNU
Norwegian University of
Science and Technology
Faculty of Engineering
Department of Mechanical and Industrial Engineering



Norwegian University of
Science and Technology

Digital Twin Modelling of High Voltage DC Generator

Hilde Nordvik

Mechanical Engineering

Submission date: June 2019

Supervisor: Terje Rølvåg

Co-supervisor: Pål Keim Olsen

Norwegian University of Science and Technology
Department of Mechanical and Industrial Engineering

Preface

This paper concludes a master thesis written as a part of the MSc degree at the Norwegian University of Science and Technology. The work has been carried out at the Department of Mechanical and Industrial Engineering during the course of spring 2019. Supervisors of this project are Professor Terje Rølvåg and Pål Keim Olsen.

I would like to thank Professor Terje Rølvåg for the opportunity and guidance throughout the two semesters of cooperation. I would also like to thank Pål Keim Olsen for his helpful input and encouragement throughout the project. Thereafter I would like to thank Magnus Borgersen and Marta Karoline Husebø for the cooperation and valuable discussions during the course of this project, it was of great help.

Trondheim, 2019-06-11



Hilde Nordvik

Abstract

This master thesis is executed as a part of the first phase of the ModHVDC project, which is development of concept and technology. The ModHVDC project aims to develop a modular HVDC generator which matches the future power grids and supports current battery storage of AC producing energy sources. This work is a contribution to the mechanical design of the segmented generator.

Coupled analyses were executed by utilising ANSYS multi-physics simulation platforms. Thermal and electromagnetic analyses were coupled through ANSYS Workbench, with the use of the platforms Maxwell and Mechanical. In order to benchmark the results, a simplified thermal circuit of the generator was developed. Thereafter, work on digital twin monitoring of the ModHVDC generator was initiated. The possibilities and applications of the multidisciplinary ANSYS digital twin concept, Twin Builder, was studied and tested. Simulation results were used to create a FMU relating generator speed and temperature, similar to the previous work done with GE Haliade wind turbine and PTC electric motor. At last, the thermal solvers in NX Nastran, SOL 153/159, were studied and tested for use in similar projects.

The two load cases in the thermal analyses resulted in maximum temperatures of 123 °C and 99 °C. This result is highly dependent on the applied convection coefficient which was defined in the lower range in these analyses. By increasing the convection coefficient on the outer faces of the stator, the temperature decreased significantly. The thermal benchmark resulted in a maximum temperature of 74 °C. Several simplifications were made creating the circuit and the FEA results are thus considered to be within a reasonable range. A top-down framework for digital twin monitoring is suggested. Temperature and vibration were found as the most critical failure modes and must therefore be the focus in further development of the digital twin. The FMU file were successfully implemented in Twin Builder schematics tracing the key parameters. ANSYS Twin Builder still lacks some key features to create digital twins and is concluded to be premature at this stage. Previous work is assumed to be performed on beta versions still not available. The ModHVDC project is still in an early face and will be continued in following master theses.

Sammendrag

Denne masteroppgaven er utført som en del av konsept- og teknologiutviklingen i første fase av ModHVDC-prosjektet. Prosjektet tar sikte på å utvikle en modulær HVDC-generator som samsvarer med det fremtidige strømmettet og støtter dagens batterilagring av vekselstrømskilder. Arbeidet er et bidrag til det mekaniske designet av den segmenterte generatoren.

Koblede analyser ble utført ved hjelp av ANSYS sine simuleringsplattformer. Termiske og elektromagnetiske analyser ble koblet gjennom ANSYS Workbench, med bruk av plattformene Maxwell og Mechanical. En forenklet termisk krets ble utviklet for å validere de termiske resultatene. Deretter ble arbeidet med å utvikle en digital tvilling satt i gang. Muligheter og bruksområder med ANSYS sitt tverrfaglige konsept for digitale tvillinger, Twin Builder, ble studert og testet. Analyseresultatene ble brukt til å lage en FMU med generatorhastighet som input og temperatur som output. Dette er gjort i lignende arbeid med GE Haliade vindturbinen og PTC sin elektriske motor. Til slutt ble de termiske solverne i NX Nastran, SOL 153/159, studert og testet for bruk i lignende prosjekter.

De to lasttilfellene i de termiske analysene resulterte i maksimale temperaturer på 123 °C og 99 °C. Disse resultatene er svært avhengig av den påførte konveksjonskoeffisienten som er definert som relativ lav i disse analysene. Ved å øke konveksjonskoeffisienten på statorens ytre flater, ble temperaturen redusert betydelig. Den termiske kretsen resulterte i en maksimal temperatur på 74 °C. Flere forenklinger ble gjort i denne kretsen, og FEA-resultatene anses derfor for å være i en rimelig størrelsesorden. Et rammeverk for en digital tvilling er foreslått. Temperatur og vibrasjon ble funnet til å være de mest kritiske feilmodene, og må derfor være i fokus i videreutviklingen av den digitale tvillingen. FMU-filen ble vellykket implementert i Twin Builder for overvåkning av de viktigste parameterne. ANSYS Twin Builder mangler fortsatt viktige funksjoner for å utvikle digitale tvillinger, og konkluderes derfor for å være prematurt på dette stadiet. Tidligere arbeid er antatt å være utført på beta-versjoner som ikke er tilgjengelig enda. ModHVDC-prosjektet er fortsatt på et tidlig stadium, og skal fortsettes på i påfølgende masteroppgaver.

Table of Contents

Preface	i
Abstract	iii
Sammendrag	v
Table of Contents	ix
List of Tables	x
List of Figures	xii
Abbreviations	xiii
1 Introduction	1
1.1 Background	1
1.2 Problem Formulation	2
1.3 Project Scope	2
1.3.1 Objectives	2
1.3.2 Approach	3
1.3.3 Limitations	3
1.4 Outline	3
2 Theory	5
2.1 The ModHVDC Technology	5
2.2 Digital Twin	7
2.3 ANSYS Twin Builder	8
2.3.1 Functional Mock-Up Interface	10
2.3.2 Co-Simulation and Reduced-Order Modelling	11
2.4 Siemens NX: SOL 153/159	12
2.4.1 Thermal Loads and Boundary Conditions	12
2.4.2 Coupled thermo-structural analysis	14
2.5 Thermal Analysis	14
2.5.1 Convection	15

2.5.2	Thermal Circuit	15
2.6	Monitoring of Electric Machines	17
2.6.1	Methods	17
2.6.2	Failure Modes	18
2.6.3	Accelerometer	19
2.6.4	Fast Fourier Transform	20
3	Previous Work and Literature	21
3.1	GE Haliade Wind Turbine	21
3.2	PTC Motor and Pump System	22
3.2.1	Pump	22
3.2.2	Electric Motor	23
4	Model	25
4.1	ANSYS	25
4.1.1	Materials	26
4.1.2	Mesh	27
4.2	NX	28
4.2.1	Materials	28
4.2.2	Mesh	28
4.2.3	Mesh Mating	29
5	Finite Element Analysis in ANSYS	31
5.1	Workflow	31
5.2	Coupling of NX and ANSYS	33
5.3	Workbench Setup	34
5.4	Electromagnetic Analysis	34
5.5	Thermal Analysis	35
5.5.1	Method	35
5.5.2	Boundary Conditions	36
5.5.3	Simulation	38
5.6	Optimetric Analysis	38
5.6.1	Parameter Set	38
5.6.2	Response Surface	38
6	Thermal Analyses in NX Nastran	41
6.1	Thermal - SOL 153	41
6.1.1	Boundary Conditions	41
6.2	Coupled - SOL 101	42
7	Thermal Benchmark	45
8	Analysis Results	49
8.1	ANSYS	49
8.1.1	Steady-State Thermal	49
8.1.2	Response Surface	51

8.2	NX	52
8.2.1	SOL 153	52
8.2.2	SOL 101	53
8.3	Thermal Circuit	54
9	Digital Twin Solution	57
9.1	Digital Twin Applications of the ModHVDC Generator	57
9.1.1	Performance Monitoring	58
9.1.2	Temperature Monitoring	58
9.1.3	Vibration Monitoring	58
9.2	Framework for Digital Twin Monitoring	59
9.3	FMU Implementation	60
10	Discussion	63
10.1	Challenges	63
10.2	Analyses	64
10.2.1	Simplifications	64
10.2.2	Communication between NX and ANSYS	64
10.2.3	ANSYS	64
10.2.4	NX	65
10.2.5	Thermal Benchmark	65
10.3	Digital Twin Monitoring	66
10.3.1	Failure Modes	66
10.3.2	FMU Creation	66
10.3.3	ANSYS Twin Builder	67
11	Conclusion and Further Work	69
11.1	Summary and Conclusions	69
11.2	Further Work	70
	Bibliography	71
	Appendix	74
A	Material Properties	74
B	PM Generator Configurator	76
C	Electromagnetic Analysis in ANSYS Maxwell	78
C.1	Requirements	78
C.2	Finite Element Analysis	79
C.3	Winding Layout	81
C.4	Heat Generation from ANSYS Maxwell	82
D	Modal Analysis	86

List of Tables

2.1	Advantages and disadvantages with ROM and co-simulation methods in Twin Builder.	12
2.2	Settings for structural and heat transfer combinations.	14
2.3	Thermal-electrical analogous quantities.	15
4.1	Machine data of the generator model	26
4.2	Material assignment of the generator used in ANSYS.	26
4.3	Mesh properties of generator in ANSYS.	27
4.4	Material assignment of the generator used in NX.	28
4.5	Mesh properties of generator in NX.	29
5.1	Properties of the applied boundary conditions in ANSYS Mechanical. . .	36
6.1	Properties of applied boundary conditions in NX.	41
7.1	Constants used in thermal circuit.	47
7.2	Resulting thermal components.	47
8.1	Resulting temperature with varying convection coefficient.	50
8.2	Resulting design of experiment.	52
8.3	Resulting temperatures from thermal circuit.	54
9.1	The key parameters to monitor in a generator	57
A.1	Material properties for electromagnetic analyses in ANSYS Maxwell. . .	74
A.2	Material properties for analyses in ANSYS.	74
A.3	Material properties for analyses in NX.	75
C.1	Machine data of the prototype generator	78
C.2	Imported Load Transfer Summary.	82
D.1	Resulting modal frequencies.	87

List of Figures

2.1	Simplified electric conversion system concept of ModHVDC.	6
2.2	The reduction of LCOE for ModHVDC technology applied to onshore wind compared to major energy sources.	7
2.3	Available load types in NX Nastran thermal analyses.	13
2.4	Available constraint types in NX Nastran thermal analyses.	14
2.5	Thermal flow through a plane wall.	16
3.1	Workbench integration between Maxwell and thermal analysis in GE's Haliade project together with the input and output parameters.	21
3.2	ROM integration in ANSYS Twin Builder used for predicting the remaining motor lifetime based on temperature.	22
3.3	The digital twin in ANSYS Thingworx.	24
4.1	Model of segmented generator used in ANSYS analyses.	25
4.2	Meshing of segmented generator. Rotor and magnets are suppressed. . .	27
4.3	The two models used for thermal and coupled analyses in NX. Different concepts of fastening.	28
4.4	Meshing of the two generator segments.	29
4.5	Mesh mating of the two models.	29
5.1	Overview of project approach.	31
5.2	Workflow and communication between software.	32
5.3	Integration of NX geometry into ANSYS Maxwell.	33
5.4	Setup of coupled thermal analyses in ANSYS Workbench.	34
5.5	Overview of thermal analysis approach.	35
5.6	Convection defined on all external faces exposed to surrounding air. . . .	36
5.7	Imported load from ANSYS Maxwell.	37
5.8	The two load cases analysed in ANSYS Steady-State Thermal.	37
5.9	Parameters gathered in the Parameter Set in ANSYS Workbench.	38
5.10	Response Surface interface in ANSYS Workbench.	39
5.11	Design points of Design of Experiment.	39
6.1	Convection defined on the model.	42
6.2	Internal heat generation applied to the model.	42

6.3	Initial temperature applied in a temperature set.	43
6.4	Temperature load imported to the temperature set.	43
6.5	Boundary conditions in coupled thermal and structural analyses in NX. . .	44
7.1	Geometry in equivalent thermal circuit.	45
7.2	Thermal resistors of each component.	46
8.1	Temperature distribution from load case 1 - ANSYS Steady-State Thermal.	49
8.2	Temperature distribution from load case 2 - ANSYS Steady-State Thermal.	50
8.3	Maximum temperature in the windings over convection coefficient on outer faces.	51
8.4	Minimum temperature in the windings over convection coefficient on outer faces.	51
8.5	Generated response surface showing temperature over velocity.	52
8.6	Temperature results on concept 1 - SOL 153.	53
8.7	Temperature results on concept 2 - SOL 153.	53
8.8	Displacement results on concept 1 - SOL 153/101.	54
8.9	Resulting thermal circuit created in LTSpice.	55
9.1	Digital Twin Architecture.	59
9.2	Framework for Digital Twin monitoring.	60
9.3	FMU implemented in ANSYS Twin Builder.	60
9.4	Data set implemented as input to the FMU.	61
9.5	Resulting trace of temperature as a function of generator speed.	61
A.1	B-H curve for Steel 1008 and M400-50A.	75
B.1	PM Generator Configurator: Example configuration with stator fastening concept 1.	76
B.2	PM Generator Configurator: Generator Configuration.	77
B.3	PM Generator Configurator: Stator Fastening Concept.	77
C.1	2D section of the generator used in analyses performed in ANSYS Maxwell.	80
C.2	Winding layout for the analysed generator.	81
D.1	Generator model used in modal analyses.	86

Abbreviations

AC	Alternating Current
CAD	Computer-Aided Design
CFD	Computational Fluid Dynamics
DC	Direct Current
ECE	Equivalent Circuit-Extraction
FEA	Finite Element Analysis
FFT	Fast Fourier Transform
FMI	Functional Mock-Up Interface
FMU	Functional Mock-Up Unit
HMI	Human Machine Interface
HVDC	High Voltage Direct Current
IIoT	Industrial Internet of Things
ModHVDC	Modular High Voltage Direct Current
LCOE	Levelized Cost Of Energy
PM	Permanent Magnet
PTS	Product Template Studio
ROM	Reduced-Order Model
RPM	Revolutions per Minute
XiL	X-in-the-Loop

Chapter 1

Introduction

This first chapter presents the background of the project. The problem formulation and objectives of this thesis will be described, followed by the project scope. At last, the structure of the thesis is presented.

1.1 Background

In the fall of 2018 *Pål Keim Olsen* submitted the proposal *Modular High Voltage Direct Current Generator for Onshore Wind* (ModHVDC) for the EU programme *Horizon 2020*. The future EU trans-regional and trans-national power grid, the super grid, will operate at direct current for long-distance energy transportation. The current rotating generator in renewable energy sources is producing alternating current, thus requiring costly transformation steps to be connected to DC grid systems. With future electricity production shifting towards renewable energy sources, the increasing need of current battery storage will need to match the power demand. The ModHVDC project aims to develop a modular HVDC generator which matches the future power grids and supports current battery storage of AC producing energy sources.

The first phase of the ModHVDC project is concept and technology development. Development will focus on a scalable and modular HVDC generator where interdisciplinary design and cooperation are required. This includes electrochemical, thermal, mechanical, electrostatic design, as well as development of an electrical insulation system [1]. The mechanical design is performed at NTNU, and Professor *Terje Rølvåg* from the *Department of Mechanical and Industrial Engineering* is assigned the task. This master thesis is one of three theses written on the ModHVDC project during the course of spring semester of 2019. It will be a contribution to the mechanical design of the project.

1.2 Problem Formulation

The primary goal of the mechanical design task is to provide a scalable mechanical design, which includes identification of magnetic, electrostatic and thermal design drivers. In the EU proposal, the following mechanical design tasks are presented [1]:

- Identify mechanical design load cases.
- Identify scalability and modularity design drivers.
- Optimise mechanical design and structural properties based (performance and integrity criteria).
- Optimise generator segment fastening design and modularity (cost and scalability criteria).
- Parametric model of ModHVDC generator unit, including model for Digital Twin monitoring of structural integrative and predictive maintenance.
- Tolerance analysis.
- Complete mechanical design for ModHVDC demonstrator frame, bearings, shaft, stator and rotor.
- Deliver production drawings for the generator and follow up production and physical testing.
- Mechanical sensor specifications for demonstrator in industrially relevant environment.
- Vibration testing in ModHVDC demonstrator.
- Implementation and testing of Digital Twin.

1.3 Project Scope

1.3.1 Objectives

The goal of this thesis is to explore the thermal and structural design drivers, as well as explore the possibilities and applications of digital twin monitoring of the ModHVDC generator.

The main objectives of this thesis are as follows:

1. Study the multidisciplinary ANSYS digital twin concept.
2. Implement a top-down framework for digital twin monitoring of the ModHVDC generator. Focus on vibration detection and structural deflection monitoring due to structural and thermal loads. Try to embed Maxwell flux analysis if possible (as a ROM/FMU).

-
3. Establish a ROM (Response Surface ROM) relating generator speed, output power and generator heat distribution (ref. GE example).
 4. Perform coupled thermal and structural analysis in ANSYS based on the electromagnetic analysis perform in ANSYS Maxwell. Embed the simulation results in Twin Builder FMUs.
 5. Study the NX Nastran thermal solvers.

1.3.2 Approach

In total, three master students will contribute to the ModHVDC project. In addition to this master thesis, *Magnus Borgersen* from the *Department of Mechanical and Industrial Engineering* and *Marta Karoline Husebø* from the *Department of Electric Power Engineering* will write their master theses within the ModHVDC project. Magnus Borgersen's thesis will focus on the geometrical aspects of the generator and will contribute to the design and development of fastening and insulation of the generator. A geometrical model of the generator is created in Siemens NX. Marta Karoline Husebø's thesis will focus on the electromagnetic aspect of the project, and will explore the effect of segmentation. Analyses on the modular generator are performed in ANSYS Maxwell. This thesis will focus on the mechanical and thermal effects on the generator, and coupled analyses are performed in ANSYS.

1.3.3 Limitations

Generators and electric machines like the ModHVDC generator is an entirely new field for the author. Using some time to study the electromagnetic aspects and the ANSYS Maxwell software was therefore necessary before starting the project work. The majority of the project team have a mechanical background which makes it difficult to interpret the work and obtained results.

As ANSYS Twin Builder is a relatively new release, limited documentation is available. Not much resources are available on the subject and this project work therefore introduced some time-consuming challenges.

1.4 Outline

The master thesis consists of several chapters including Introduction, Theory, Previous Work, Model, Finite Element Analysis in ANSYS, Thermal Analysis in NX Nastran, Thermal Benchmark, Analysis Results, Digital Twin Solution, Discussion, Conclusion and Further Work, Bibliography and Appendices. The structure of the thesis is as follows:

Chapter 1 gives an introduction to the thesis. It describes the background of the project, as well as presenting the problem formulation, project scope and structure of the thesis.

Chapter 2 presents the relevant theory used in the thesis. This includes a introduction to the concept of digital twins, ANSYS Twin Builder, FMU creation, monitoring of electric machines and relevant analysis theory.

Chapter 3 describes the previous work done on this subject. The work done on digital twins by GE Digital on the Haliade offshore wind turbine as well as the work performed by ANSYS and PTC on a pump and electric motor system is discussed.

Chapter 4 presents the model used in the project and analyses. The material, overall requirements and meshing of the models are described.

Chapter 5 describes the analyses performed through ANSYS Workbench. The method, boundary conditions, and simulation setup are explained.

Chapter 6 presents the simulations performed in Siemens NX. The thermal solvers in NX Nastran are explored and the chapter describes the method, boundary conditions, and simulation setup.

Chapter 7 goes through the work done on an equivalent thermal circuit of the generator model. The circuit is to be used as a benchmark for the FEA results.

Chapter 8 presents the analysis results. The solutions of the analysis in both ANSYS and NX are described, as well as the results of the thermal circuit.

Chapter 9 presents the results and work done on digital twin monitoring of the Mod-HVDC generator. It describes implementation of FMUs in Twin Builder, failure modes and framework for digital twin monitoring.

Chapter 10 is the discussion chapter. Both the method and results are discussed, as well as the challenges throughout the project.

Chapter 11 is the last chapter and provides a summary of the work, results and conclusions. Suggestions for further work are also presented.

Chapter 2

Theory

2.1 The ModHVDC Technology

The ModHVDC technology is described in the project report written by Borgersen, Litlabø, Opheim and Nordvik in the fall of 2018. It is reintroduced in this section.

Pål Keim Olsen [1] describes the main concept of the ModHVDC generator to be the combination of a generator and a high voltage transformer with stacking of the converter voltages instead of the generator coil group voltages. It is a new design of the generator and electrical drive train which enables generation of HVDC power. For conventional electric machines, a generator consists of a stationary and a rotating part, i.e. stator and rotor. The ModHVDC stator is modular and each module is connected to the DC potential level of the converter. Figure 2.1, taken from [1], illustrates the electric conversion system concept of the ModHVDC generator. The ModHVDC stator core is divided into the modules MG1-MG4 where each of these modules are connected to the DC potential levels 1M-4M of the converters. The AC and DC voltage stresses inside the machine are separated for optimal distribution of voltage stresses. This means that less electric insulation is needed which results in an increase of power per weight compared to state-of-the-art conventional machines.

Another direct benefit of the ModHVDC technology is that today's use of low voltage/high current to high voltage/low current transformers will be eliminated, as these stages now will be performed in the wind turbine's nacelle. Today, these transformer steps introduce efficiency losses up to 2%. At a system scale, the construction, management and maintenance of the transformers introduces a large capital investment when planning new energy plants. Eliminating these stages will therefore reduce the capital expenditure, CAPEX, for ModHVDC power plants. CAPEX is defined as the expenses a company uses to upgrade or acquire its assets, such as property, buildings, vehicles and equipment.

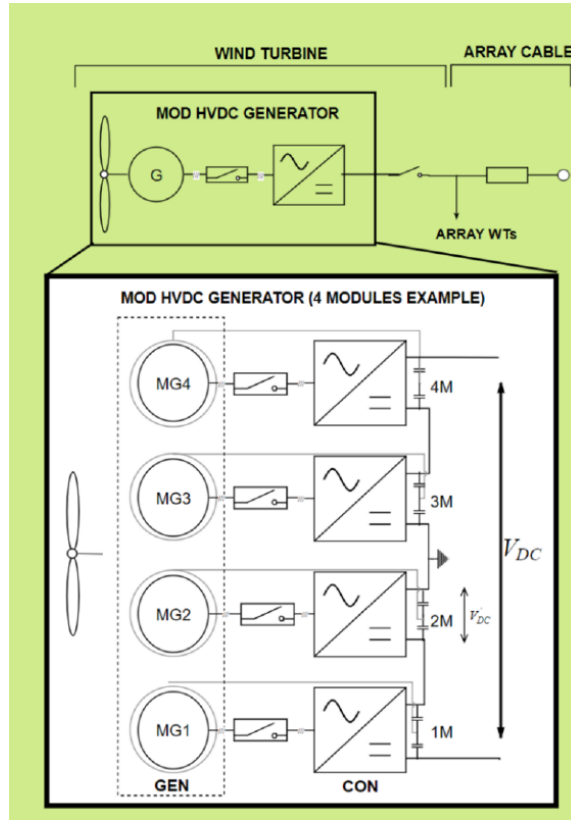


Figure 2.1: Simplified electric conversion system concept of ModHVDC.

Preliminary calculations indicates at least a 10% reduction of LCOE with integration of ModHVDC technology [1, Part B, Section 2]. Levelised Cost of Energy (LCOE) is a measure that enables consistent comparison of different methods to generate electricity. It is calculated by taking the average total cost of building and operating a power-generating asset over its total lifetime, divided by the total energy output of the asset over that lifetime. Figure 2.2, taken from [1], shows the LCOE range for major energy sources compared to possible implementation of ModHVDC technology, with data taken from [2]. The calculated decrease in LCOE due to ModHVDC technology is expected to give back competitiveness of EU onshore wind compared to North American and Asian onshore wind.

Today, hydro power and wind power are the two main renewable energy sources. The ModHVDC technology will target wind power due to capacity growth limitations in hydro power. ModHVDC technology is believed to open up for new onshore wind sites with fewer turbines distanced from residential areas. The technology is believed to enhance social acceptance of onshore wind power because of its reduced environmental footprint and reduced electricity cost.

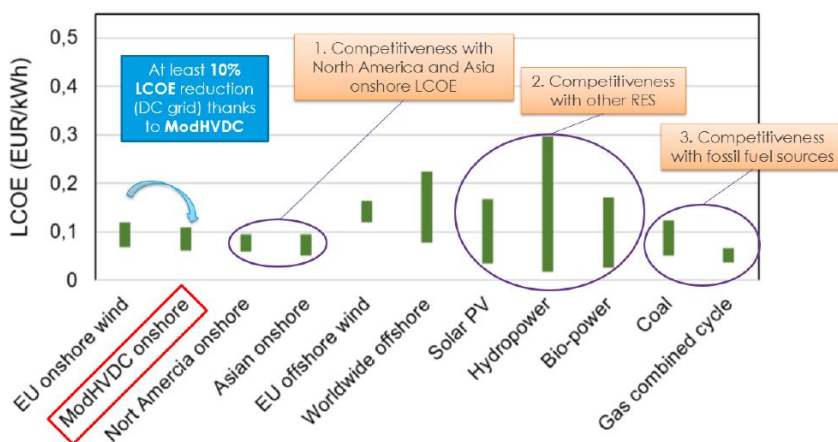


Figure 2.2: The reduction of LCOE for ModHVDC technology applied to onshore wind compared to major energy sources.

The main advantages of the ModHVDC technology can be summarised as:

- Theoretical calculations indicate a 75-90% reduction of equivalent slot insulation thickness in the stator compared to state-of-the-art conventional high voltage machines.
- Same power per weight as state-of-the-art machines, at 4-10 times the voltage output.
- Modularity of the ModHVDC stator increases manufacturability and ease of assembly.
- Decrease in LCOE for onshore EU wind by implementing ModHVDC technology, making onshore wind energy competitive with fossil fuel sources, as well as other renewable energy sources.

2.2 Digital Twin

Simulation in system development has developed tremendously in the last decades. It has gone from being limited to experts to being used daily by engineers in design and engineering. The number of users started to grow in the 1980s-1990s and simulation became a standard tool to answer specific cases. Now simulation allows a systematic approach to multilevel and multidisciplinary systems and is a crucial step in design, validation and testing. The Digital Twin is the next wave in simulation technology. Simulation will then be important throughout the life cycle, e.g. supporting operation and service with direct linkage to operation data [3].

A digital twin is a digital representation of a physical object, asset or system. It is connected to the real asset with the use of sensors, network and IIoT devices. An ideal digital twin will contain information on all the parameters possible to measure from the physical object. The twin will retrieve information on the history of the asset, and will thus be unique for this particular asset. GE Digital [4] defines a digital twin as a digital model of an industrial asset, e.g. a jet engine or a wind turbine. By collecting data from physical and virtual sensors and analysing this data, a digital twin will gain insights about performance and operation of the assets. GE Digital further presents the benefits of the digital twin technology as :

- Increased reliability and availability
- Reduced risk
- Lower maintenance costs
- Improved production
- Faster time-to-value

According to ANSYS [5] a simulation-based digital twin is a "connected, virtual replica of an in-service physical asset in the form of an integrated multi-domain system simulation that mirrors the life and experience of the asset". The digital twin enables predictive and prescriptive maintenance and optimises industrial asset management . Companies can use digital twins to detect faults, perform diagnostics, recommend corrective action, determine maintenance schedule, optimise asset operation and generate insights that can improve the product's next generation.

The objective regarding digital twin technology for this project is to investigate the possibilities of creating and monitoring a digital model of the ModHVDC generator. Chapter 9 presents the work done on digital twin monitoring.

2.3 ANSYS Twin Builder

With the release of ANSYS Version R19.1 in 2018, ANSYS introduced a new product named *Twin Builder*. Twin Builder is a continuation of the previous multi-domain system simulation program ANSYS Simplorer. It will include existing technology such as SCADE and reduced order modeling (ROM). ANSYS [6] describes the objective of the Twin Builder as "Build, Validate and Deploy Complete Systems Simulations and Digital Twins for Predictive Maintenance".

With Twin Builder, ANSYS reach to obtain savings on warranty and insurance costs, optimisation of product operations and implementing of predictive maintenance. The software allows to build systems, validate and ensure expected performance, and to connect digital twins to test or real-time data. Predictive maintenance is enabled by the connection to IIoT platforms. The workflow is divided into the three stages build, validate and deploy.

Build

The first step is to build the digital twin. By doing a failure mode analysis one can determine which kind of digital twin is needed. With the use of techniques like reduced order modelling and behavioural modelling existing simulation models used during design can be used to create and build an accurate digital twin of the asset. The use of Twin Builder is intended to reduce engineering time with reuse of models and easy composition with [7]:

- Support for multiple modelling domains and languages. Schematics of complex power electronic circuit and multi-domain system can be created with standard languages and exchange formats like VHDL-AMS, Modelica, SML, FMI, C/C++ and Spice.
- Extensive 0D application-specific libraries. Twin Builder libraries include analogue and power electronics components; control blocks and sensors; mechanical components; hydraulic components; digital and logic blocks; application-specific libraries for aerospace electrical networks, electric vehicles and power systems; and characterised manufacturers components. Support for the Modelica Standard Library and Modelica libraries offered by Modelon AB is included.
- Third-party tool (including 1D) integration is enabled with support of the FMI standard. Over 100 tools supports FMI model export, including GT-SUITE, CarSim, Amesim and Dymola. Integration of C/C++ code and Mathworks Simulink model is also supported. Twin builder models can further be exported with the use of FMI.
- 3D ROM creation and integration. ROMs generated from ANSYS structural, fluids, electromagnetics and semiconductor products can generate accurate and efficient system-level models from detailed 3D simulations. Co-simulation with 3D solvers enables full accuracy of FEA and CFD in system simulation.
- Embedded software integration. Support of model-in-the-loop and software-in-the-loop flows with embedded control software and HMI design for testing of performance of embedded controls with models of the physical system.

Validate

The second step is to validate the digital twin. By tuning and optimising parameters, the digital twin is validated to an accurate representation of the asset. Product performance can be optimised with the use of [7]:

- Multi-domain simulation with integrated post-processing. Accurate simulation of continuous-time, discrete-time and analogue/mixed-signal behaviours with adaptive time-step controls and solver synchronisation capabilities. Graphical waveform plotting, graphical and tabular reports and a large collection of predefined measurements and markers gives a complete environment for post-processing simulation results.

-
- Rapid HMI prototyping enables powerful and easily designed panels with predefined widgets.
 - System optimisation with basic simulation experiments and an advanced testing suite. Parameter values can be swept to understand the system response.
 - XiL integration. Co-simulation for model-in-the-loop (MiL) design and tuning of control strategies, and code import for software-in-the-loop (SiL) validation of the real embedded code in the virtual system.

Deploy

Lastly, the models can be deployed and connected to the several IIoT platforms available. This allows connecting of the models to real-time data, and deployment of the digital twin at scale. This is done by [7]:

- Quick connection to supported IIoT platforms like PTC ThingWorx, GE Predix, SAP Leonardo and homegrown varieties.
- Export and deploy generated models.

2.3.1 Functional Mock-Up Interface

The Functional Mock-up Interface (FMI) is a standard for exchanging system models, emphasising portability, interoperability, and deployability within the enterprise. A component which implements the FMI is called a Functional Mock-up Unit (FMU). A FMU is intended to be a portable, dynamic simulation model for exchange or co-simulation. It is a zipped file (.fmu) that contains:

- Interface description (XML)
- Model functionality (C-code, either as source or binary)
- Additional data (e.g. tables, maps) and functionality.

The advantage of the FMU is that the full set-up of the analysis and model can be shared with others, meaning that detailed knowledge of setting up analyses for one model is not needed when receiving the FMU. The FMU serves as a "black box", where the user defines its own inputs and get a corresponding output by using interpolation techniques to extract the relevant data from the response surface. The FMU is usable in a co-simulation workflow, e.g. Twin Builder. FMU can be created with any tool supporting the FMI standard. The FMU technology is utilised in this project and implemented in the Twin Builder schematics.

2.3.2 Co-Simulation and Reduced-Order Modelling

ANSYS defines a ROM as "compact, computer generated numerical representations of high-fidelity (3D) models that preserve essential behaviour and dominant effects". The applications are further presented as

- Speed up 3D simulation (ROM for 3D).
- Performing efficient system simulation (ROM for systems).
- Support non-traditional users to explore the design space (ROM for simulation democratisation).
- As physical plant models in the design, verification and operations of control systems to enhance their precision (ROM for control design).

ROM is a valuable tool for linking 3D models to 0D systems like Twin Builder, and allows the analyses performed in physics tool be controlled by the schematics in Twin Builder. This further allows connection of co-simulations from other domains. There are three main methods for ROM creation of interest: Response Surface ROM, Static ROM Builder and Equivalent Circuit Extraction (ECE). These methods are further explained below. In this project, the Response Surface ROM is utilised for creation of FMU components. The pros and cons of ROM and co-simulation methods are summarised in Table 2.1, taken from the project report.

- Response Surface ROM: Creation of a response surface and exporting it as a ROM or FMU. The user defines input and output parameters, and a sweep of the input parameter results in a response surface. When defining n parameters, a n -D response surface is created for every output parameter by doing a parameter sweep over all input parameters.
- Static ROM Builder: Currently (ANSYS R19.2) only available for ANSYS Fluent. Multiple simulations of varying input parameters used to export a ROM or FMU.
- Equivalent Circuit Extraction (ECE): Used for Maxwell analyses. Creates a co-simulation and a dynamic link between Maxwell and Twin Builder. Maxwell produces a look-up table (for example current vs. rotor angle/position) and an equivalent circuit matrix. The ECE model can then be imported into Twin Builder for analysis.

	Pros	Cons
Co-simulation	Exact solution. Possibility to control analysis settings in the models. Multiple solver domains can be coupled.	Slow solution process. Knowledge of setting up simulations required.
Response surface	Fast interpolation of solutions. Can be exported as FMU or ROM.	Slow creation of response surface. Not exact solution (interpolated).
Static ROM builder	Has its external viewer - the ROM Viewer. Can be exported as a FMU.	Only for ANSYS Fluent. Poorly documented.
ECE extraction	Fast solution (from look-up table). Imports directly into Twin Builder. Possibility to control analysis settings in the models.	Only possible for magneto-static solution types. No exact solution (interpolation from look-up table).

Table 2.1: Advantages and disadvantages with ROM and co-simulation methods in Twin Builder.

2.4 Siemens NX: SOL 153/159

NX Nastran offers a variety of different solvers, both linear and nonlinear. Among these are linear static analysis (SOL 101), eigenfrequency and free vibration mode analysis (SOL 103), time and frequency response analysis (SOL 108, 109, 111, 112), structure buckling analysis (SOL 105), basic nonlinear analysis (SOL 106) and transient process analysis (SOL 129). In addition to the structural solvers, NX Nastran offers thermal and acoustic solvers. Two types of heat transfer problems, steady state and transient analysis, are solved by NX Nastran [8]. SOL 153 is the steady state heat transfer solver for linear and/or nonlinear problems. SOL 159 is the transient heat transfer solver for linear and/or nonlinear problems.

The solvers implemented in this master thesis are SOL 153 and SOL 101.

2.4.1 Thermal Loads and Boundary Conditions

NX Nastran clearly distinguishes between loads and boundary conditions. Figure 2.3 shows the loads possible to choose. The available thermal loads in SOL 153 and SOL 159 are:

- Directional heat flux from a distant source.

-
- Volumetric internal heat generation.
 - Heat flux applied to an area defined by grid points.
 - Heat flux applied to surface elements.
 - Heat flux applied to grid points associated with a surface element.
 - Heat flux applied to surface elements with control node capability.
 - Power into a grid or scalar point.
 - Nonlinear transient load as a tabular function.
 - Nonlinear transient load as a product of two variables.
 - Nonlinear transient load as a positive variable raised to a power.
 - Nonlinear transient load as a negative variable raised to a power.

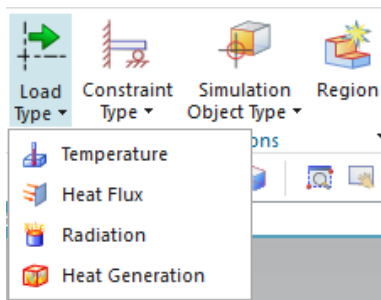


Figure 2.3: Available load types in NX Nastran thermal analyses.

Figure 2.4 shows the boundary conditions possible to choose. NX Nastran treats the application of radiation and convection as boundary conditions. The available boundary conditions in SOL 153 and SOL 159 are:

- Free convection heat transfer coefficient.
- Forced convection (fluid "element").
- Radiation exchange with space.
- Radiation exchange within an enclosure.

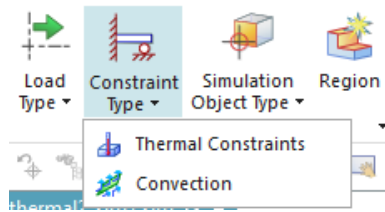


Figure 2.4: Available constraint types in NX Nastran thermal analyses.

2.4.2 Coupled thermo-structural analysis

There are two forms of coupling between thermal and structural analyses in advanced nonlinear solution. One-way coupling will import the thermal solution into the structural solution, but not the other way around. The solutions are solved separately, and thermal results can be used to calculate thermal expansion and temperature-dependent material properties. With a two-way coupling, the thermal and structural solutions are interdependent. Structural results can be used to calculate internal heat generation due to plastic deformations of the material, heat transfer between contacting bodies, and surface heat generation due to friction on the contact surfaces [9].

Table 2.2: Settings for structural and heat transfer combinations.

Structural	Heat transfer	SOL
Static	Steady	153
Static	Transient	159
Dynamic	Steady	159
Dynamic	Transient	159

Coupling can be between any combination of static or implicit dynamic structural analysis, and steady state or transient heat transfer analysis. The required heat transfer solvers are listed in Table 2.2 [9].

2.5 Thermal Analysis

Temperature is a dimensioning factor in designing electric machines, and overheating and maximum temperature are important when deciding the electric and magnetic loading of the machine. Too high temperatures inside the generator can cause magnets to demagnetise and damage to winding insulation. Performing thermal analyses is thus a crucial step in designing a generator like the ModHVDC generator. This section describes some factors needed in such analyses.

2.5.1 Convection

Convection describes the energy transfer between a surface and a fluid moving over the surface. When there is no forced velocity, convection will occur due to buoyancy forces within the fluid. This is referred to as natural convection. Natural convection originates from a fluid density gradient and a body force that is proportional to the density. Usually, the density gradient comes from a temperature gradient and the body force comes from the gravitational field [10].

The heat transfer coefficient is often based on empirical values. In the case of non-forced flow, when heat transfer occurs by natural convection, h-values will be considerable lower than by forced flow. Transfer between solid wall and gas will give h-values in the range of 5-12 W/(m² °C), while transfer between solid wall and water will give values in the range of 175-350 W/(m² °C).

Jürges [11] presented in 1924 the following empirical correlations for the convection coefficient:

$$c < 5 \text{ m/s} : \quad h = 5.6 + 4.0c \quad (2.1)$$

$$c > 5 \text{ m/s} : \quad h = 7.1C^{0.78} \quad (2.2)$$

where c in the free-stream air speed. For the analyses performed in this thesis, a convection coefficient of 6 W/(m² °C) has been used.

2.5.2 Thermal Circuit

Thermal circuits can be used to model heat flow in the same way electrical circuits are used for current flow. The thermal-electrical analogy is defined in Table 2.3 [10].

Table 2.3: Thermal-electrical analogous quantities.

	Thermal	Electrical
Through variable	Heat transfer rate, q [W]	Current, i [A]
Across variable	Temperature, θ [°C]	Voltage, V [V]
Dissipation element	Thermal resistance, R_{th} [°C/W]	Electrical resistance, R_{el} [Ω]
Storage element	Thermal capacitance, C_{th} [J/°C]	Electrical capacitance, C_e [F]

For the use in this project, it is necessary to calculate the heat generation in the windings. The heat generation per unit length is given by

$$\frac{q}{l} = J^2 \frac{A_{cu}}{\delta_{el}}, \quad (2.3)$$

where J is the current density in the windings, A_{cu} is the area of the copper, and δ_{el} is the electrical conductance of copper.

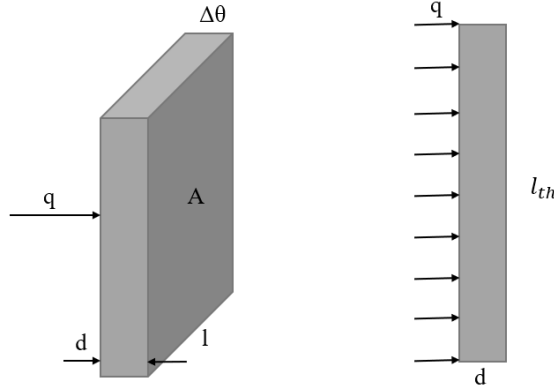


Figure 2.5: Thermal flow through a plane wall.

Thermal resistance gives the relation between the temperature difference and the conduction of heat. For a plane wall as seen in Figure 2.5, the thermal resistance is given by

$$R_{th} = \frac{\Delta\Theta}{q} = \frac{d}{kA}, \quad (2.4)$$

where d is the thickness, k is the thermal conductivity and A is the area of the wall. The thermal resistance for convection is

$$R_{th,conv} = \frac{\Delta\Theta}{q} = \frac{1}{hA}, \quad (2.5)$$

where h is the heat transfer coefficient and A is the area of the wall [10].

In order to consider a 2D heat flow system, one must calculate the thermal properties per unit length. The thermal resistance is then given by

$$R_{th} = \frac{\Delta\Theta}{q} = \frac{d}{kl_{th}}, \quad (2.6)$$

where l_{th} is defined in Figure 2.5. Similarly, the thermal resistance for convection per unit length is given by

$$R_{th,conv} = \frac{\Delta\Theta}{q} = \frac{1}{hl_{th}}. \quad (2.7)$$

2.6 Monitoring of Electric Machines

2.6.1 Methods

The main groups of fault detection are mechanical and electromechanical. Temperature, oil particle, gas analysis and performance and visual methods are also common. A combinations of these types of fault detection must be used in order to detect the varied failures. Observing the condition of the motor is applied for fault detection and as a basis for maintenance planning. According to Thorsen and Dalva [12] the main methods for condition monitoring are:

- **Performance Monitoring** by measuring parameters like supply voltage and current, input- and output power, and mechanical stress in couplings.
- **Vibration Monitoring** by measuring parameters like displacement, velocity and acceleration, radially or axially. This can be done using accelerometers further explained in Section 2.6.3. The accelerometers are often placed on the bearings to detect mechanical faults. By placing sensor on the stator as well, problems like non-even air-gap, stator winding or rotor faults, asymmetrical power supply, and imbalances in the machine load can be detected.
- **Shock Pulse Monitoring (SPM)** detects shock waves on the bearings caused by impact between moving parts and defect parts, a crack on the inner/outer race or on the rolling elements in the bearing. Piezoelectric transducers mounted to the bearings can detect these shock waves.
- **Acoustic Emission Monitoring** detects waves that propagate through the machine with the speed of sound caused by contact between rolling elements with and without cracks. Ultrasonic, as well as audible, frequencies are deployed.
- **Speed Fluctuations Monitoring** by measuring fluctuations in the rotational period of the motor. Can detect rotor faults, vibrations, air-gap eccentricity, rotor asymmetry, damaged bearings/couplings, and misalignment.
- **Current Monitoring** by analysing the motor's supply current.
- **Air-Gap Torque Monitoring** can detect cracked rotor bars and shorted stator coils.
- **Instantaneous Stator Power Monitoring** monitoring current magnitude, voltage and phase shift between current and voltage wave forms.
- **Magnetic Field Monitoring** by monitoring the axial leakage flux to identify various asymmetries and fault conditions.
- **Temperature Monitoring** can give useful information on possible friction problems in bearings. Coolant bulk temperature is often monitored. With the use of thermocouples and thermistor the temperature can be monitored.
- **Visual Monitoring** by inspection with bare eye, camera, or video tape to record trends.

2.6.2 Failure Modes

Thorsen and Dalva [12] found the most common failure reasons to be bearing faults initiated by mechanical breakage and overheating. The failure contributors are high vibration and poor lubrication. Typical mechanical breakage are damaged ball bearings, mechanical misalignment, abnormal rotor unbalance and eccentricity, shaft whirl and resonant torsional vibration. The second most common failure reason is faults on the stator windings initiated by insulation breakdown, mechanical breakage and electrical fault or malfunction. Normal deterioration from age, abnormal moisture and high moisture contributes to this type of failure.

According to Kadanik [13], the most common reason for failure in AC motors is overheating. Insulation breakage due to overheating stands for between 1/3 and 1/2 of all motor failures. It is often caused by excessive voltage or current stress. Operating at high torques and low speed, the efficiency of the internal fan drops and cannot cool the motor as well at lower speeds. This results in higher temperatures. Harmonics in the motor caused by the AC drive can result in extra heating in the copper conductors and the iron due to eddy currents. High frequency harmonics in the motor current can cause overheating in some types of rotor bars [13].

In the project report a study of the relevant parameters to monitor on the ModHVDC generator was executed. The study is reintroduced in this section as it is highly relevant for creating a framework for digital twin monitoring.

In order to optimise performance and maintain reliability and longevity of the ModHVDC generator, it is vital to monitor its key parameters. Sensor data from the generator provides the ability to diagnose problems at an early stage in their progression, while historical data provides a history of the performance of a machine and can be used for long-term trending and maintenance management. The key parameters to monitor according to Klempner [14] are summarised in the following sections.

Generator Output Power

The generator's output power is the real power output in MW from the generator. The power outputs are monitored by voltage and current signals taken from the generator potential and current transformers. Exceeding rated output power is the main concern, as it leads to high stator currents affecting the condition of the stator windings. The consequence is that the windings will overheat. This heat production may also be transferred to the stator core. The heat will have an effect on the magnets on the rotor as their magnetic permeability decreases at increasing temperatures, resulting in lower performance of the generator.

Stator Core and Frame Temperatures

When monitoring the stator core of a generator, temperature is one of the main indicators of a fault condition. The placement of temperature sensors is therefore important for

detecting the local temperature rises that occur in the generator. Temperature sensors are normally placed in the radial direction between the stator core laminates. Here, they are placed in the tooth centre, the core yoke below the slot bottom and at both core ends. This placement provides monitoring of the main core-heating modes: global overheating, core-end overheating and localised overheating around teeth.

Core and Frame Vibration

Magnetic pull in the air-gap will naturally produce vibration in the stator core. Vibration will be generated at twice the rotational frequency of the rotor. The vibration may cause interlaminar sliding in the laminates, as well as fatigue damage, resulting in pieces of core material breaking off and causing damage. Mounting accelerometers on the stator core gives the possibility to determine magnitude and phase of radial and tangential vibration modes. The stator core vibration will excite the frame supporting the stator, meaning that the frame's resonance frequency must be kept away from the vibration frequency. In order to correct the frame's resonance frequency, one normally adds mass to the frame to reduce its resonance frequency, or driving the natural frequency higher by stiffening the frame.

Rotor Speed

Monitoring rotor speed is useful for detecting the total generator structure's resonance frequency as the rotor will normally go through these during start-up and cool down. Monitoring rotor speed together with the frame vibration will reveal the structure's resonance frequencies. Shifts in these frequencies over time might be an indicator of a reduction in rotor stiffness due to for example a crack propagation in the rotor.

2.6.3 Accelerometer

Measuring of vibration can be done with several types of vibration transducers, e.g. eddy current probes, moving element velocity pick-ups, and accelerometers. The accelerometer is the most common and is covered in this thesis. An accelerometer measures acceleration and converts the signal into velocity or displacement. It consists of a spring-mounted mass connected with a piezoelectric element. The mass will apply a force to the element which is proportional to the acceleration level of the vibration.

There exists numerous different types of accelerometers, with different sensitivity to small vibrations. To obtain reliable results, accelerometers should be mounted measuring the main sensitivity axis, tri-axial accelerometers can also be used. Accelerometers can sustain temperatures up to about 250 °C, making them suitable for the use in electric machines such as the ModHVDC generator.

2.6.4 Fast Fourier Transform

Fast Fourier transform is an important tool in vibration analysis by effective computing of the discrete Fourier transform of a series of data samples. FFT is a common tool in signal analysis, and allows analysis of vibration amplitudes at various frequencies. This enables identifying and tracking of vibration at specific frequencies [15].

Chapter 3

Previous Work and Literature

3.1 GE Haliade Wind Turbine

Recently ANSYS and GE engineers completed a simulation-based digital twin of the GE Haliade 160-6 MW offshore wind turbine [16, 17]. Previous to the digital twin, GE used analytics to monitor the turbines. This is expensive and difficult since a operator must physically inspect the motors offshore. The digital twin was created on the yaw system consisting of seven motors. Seven digital twins were created as the seven motors are independent.

Since there are no real temperature sensors on the motors, virtual temperature sensors were created on each motor to collect the temperature data of each individual motor. Maxwell 3D and steady-state thermal analysis were used to detect the maximum temperature in the coils. The analysis setup is illustrated in Figure 3.1, taken from [16]. Many simulations were executed to detect the load case of the motors.

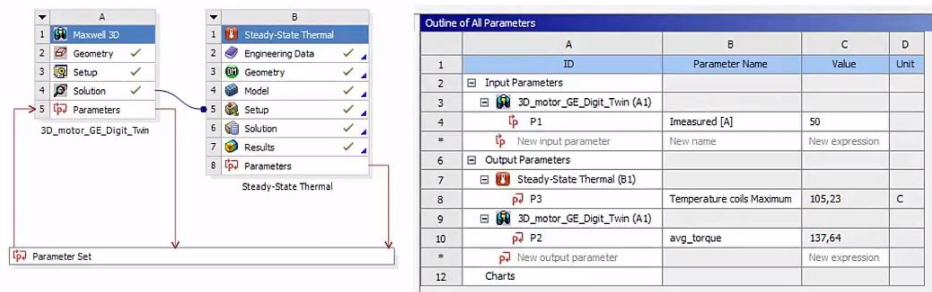


Figure 3.1: Workbench integration between Maxwell and thermal analysis in GE’s Haliade project together with the input and output parameters.

From the physics simulation, ANSYS Workbench was used to create a ROM with current as input, and torque and maximum temperature as output. This was brought into ANSYS Twin Builder for a system simulation, implementing an analytic model of the motor's remaining lifetime based on the temperature. The setup in Twin Builder is illustrated in Figure 3.2, taken from [16]. The remaining lifetime decreases as the temperature increases.

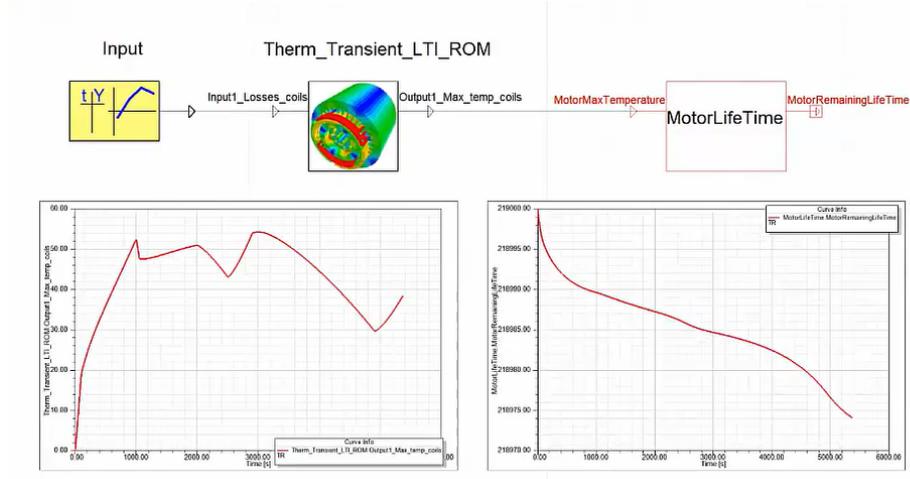


Figure 3.2: ROM integration in ANSYS Twin Builder used for predicting the remaining motor lifetime based on temperature.

The digital twin was generated using GE's own predictive maintenance system, GE Predix. Simulation of temperature and expected lifetime can now be performed for the current load situation. Information is remotely and in real time. This enables the operators to plan when to replace the motors by remotely monitoring with the digital twin.

3.2 PTC Motor and Pump System

3.2.1 Pump

In cooperation with PTC, ANSYS recently completed the work of creating a digital twin of an operating pump [18]. The pump was equipped with several sensors for monitoring of the key failure modes. This includes pressure sensors at the inlet and outlet, accelerometers on pump and bearing housings, and flow meters on the discharge side. A reduced-order, system-level model of the pump system was developed using ANSYS Simplorer. The system model and sensor data are connected through PTC ThingWorx and mimics the hydraulic system's operation. The system model also connects to a human-machine interface (HMI) developed using ANSYS SCADE software with the same gauges and dials as the

physical pump. With this configuration, the system model can be disconnected from the physical pump and operated offline to explore proposed operating scenarios.

The digital twin was deployed using the IIoT platform PTC ThingWorx®. The IIoT platform connects devices and sensors with the digital data, including the simulation model of the pump. Sensor and control data, as well as analytics, are displayed on the platform. For example, inlet and outlet pressure, and predicted bearing life are displayed on the platform. Machine learning is utilised to learn the normal state pattern of the operating pump, identify anomalies and generate insights and predictions. The IIoT platform also triggers alerts and performs predictive analytics to indicate projected life in the case of anomalies.

The system model can be instrumented using virtual sensors to measure, for example, pressure downstream and upstream of the valves. A 3D computational fluid dynamic (CDF) model of the operating pump was developed. The model can be connected to the cloud and receive real-time data from the asset. By disconnecting the system model from the physical pump, the system model's HMI could be used to try various potential fixes.

3.2.2 Electric Motor

The digital twin of the pump and its valves was expanded to its motor and electric drive [19]. The physical pump is connected to the motor driven by the electrical controller. This is a multi-domain system including fluids, electromechanical, electromagnetics and thermal aspects. A digital twin can extend the life of the motor by ensuring that the motor temperature is within the desirable range while the pump operates at around its best efficiency point.

Often there are no sensors on the motor to provide information about the temperature of the motor. Guessing of the motor temperature by monitoring the input power, current and voltage is common, but this is imprecise. Temperature sensors are often costly to operate and data is frequently inaccurate or delayed. By creating virtual sensors, the need for physical sensors is reduced. The first step is to create multi-physics simulations. Two ROMs were created, one for the electromagnetic model of the motor and one for the thermal model, with voltage and current as input and temperature as output. This enables quick prediction of both the transient and future steady state temperature of the components of the motor.

Flow and pressure will affect the motor temperature. With the digital twin, these two inputs from two sensors that indicate the opening position of the two flow valves controlling flow rate through the pump, are needed to simulate the entire system. This gives insights into the operating conditions of the pump and motor. With the digital twin and the information from the two sensors on the pump, the temperatures of the motor can be determined in addition to the current, flow rate and pressure at various locations at all times.

Figure 3.3, taken from [19], shows the digital twin in PTC Thingworx. It enables monitoring of several parameters as well as alerts in case of anomalies. Through Thingworx, the 3D models of both the pump and motor can be accessed. By disconnecting the digital

twin from the physical asset, ANSYS simulations and HMI can be used to test different scenarios and operating conditions of the digital pump and motor.

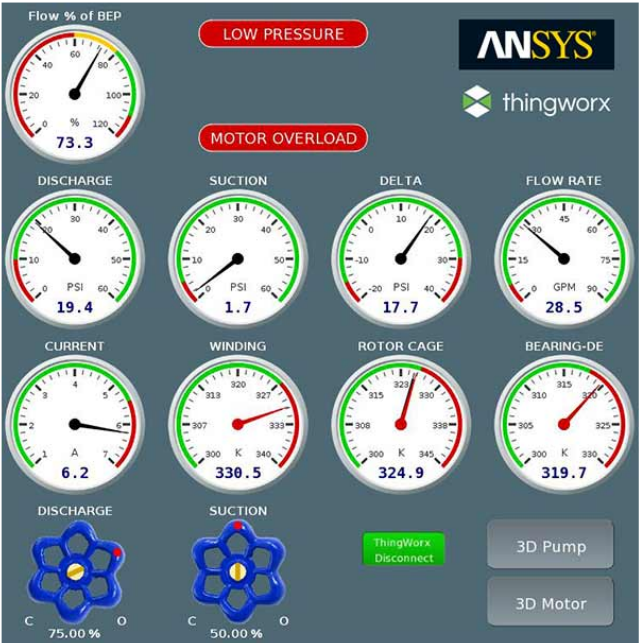


Figure 3.3: The digital twin in ANSYS Thingworx.

Chapter 4

Model

For the purpose of this project, a model of the segmented generator has been made using the Generator Configurator in NX as seen in Appendix B. The generator consists of 4 stator segments with a total of 116 poles with single-layer concentrated windings. The winding configuration can be seen in Appendix C.3. Design and creation of the generator model is described in detail in Magnus Borgersen's master thesis. This chapter present the models used in the analyses performed in ANSYS and NX.

4.1 ANSYS

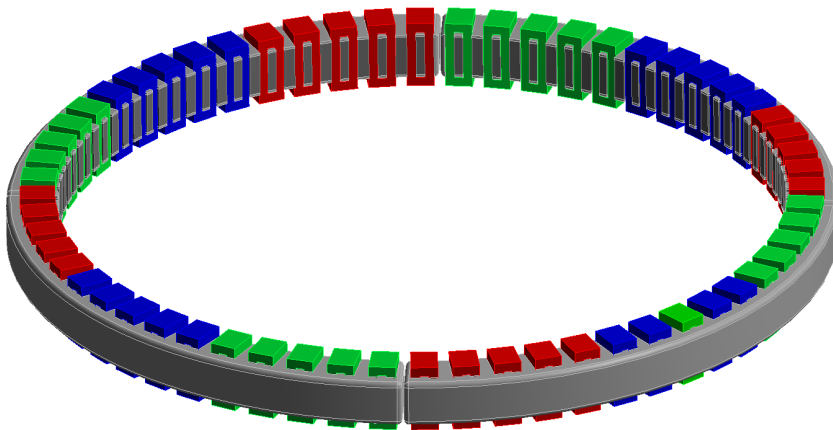


Figure 4.1: Model of segmented generator used in ANSYS analyses.

The generator model used in the ANSYS simulations is shown in Figure 4.1. Table 4.1 shows the configuration and machine data of the generator model. The model was idealised for meshing by removing edge blends and other details to reduce the run time of the analyses performed. To reduce simulation time, the rotor and magnets were excluded from the model. The generator model consist of 4 segments with insulation around the stator segments.

Table 4.1: Machine data of the generator model

Stator outer diameter	1777 mm	Number of coils	60
Stator inner diameter	1557 mm	Air-gap	5 mm
Stator depth	100 mm	Number of poles	116
Tooth width	18 mm	Number of turns	19
Stator slot depth	80 mm	Number of stator slots	120
Stator slot width	22.3 mm	Magnet height	20 mm
Number of segments	4	Magnet width	33 mm

4.1.1 Materials

The materials assigned to the generator are listed in Table 4.2. Material properties can be seen in Table A.2 in Appendix A.

Table 4.2: Material assignment of the generator used in ANSYS.

Part	Material
Coils	Copper Alloy*
Stator	Gray Cast Iron
Rotor	Gray Cast Iron
Insulation	-

Material of the insulation has not been determined. As a start, it is assumed that the insulation has a thermal conductivity of 0.1-0.3 W/mK. For the thermal analyses, a material with thermal conductivity of 0.3 W/mK was assumed.

The model created in NX have no insulation around the copper windings. In order to get a realistic result, the material properties of the copper is modified to account for the insulation. As a result, the copper windings will have a orthotropic thermal conductivity. By using Equation 2.6, the total thermal resistance in the windings are calculated as

$$R_{tot,y} = R_{cu,y} + R_{iso,y},$$

which leads to

$$\frac{1}{k_{tot,y}} \frac{\frac{1}{2}l_{cu} + d}{b_{cu} + 2d} = \frac{1}{k_{cu}} \frac{\frac{1}{2}l_{cu}}{b_{cu}} + \frac{1}{k_{iso}} \frac{d}{b_{cu}}.$$

By solving for $k_{tot,y}$ and repeating the procedure for $k_{tot,x}$, the resulting thermal conductivity is

$$\begin{bmatrix} k_{tot,x} \\ k_{tot,y} \end{bmatrix} = \begin{bmatrix} 2.90 \\ 9.86 \end{bmatrix}.$$

4.1.2 Mesh

For structural and thermal analyses, the model are meshed in ANSYS Mechanical. Mesh properties were assigned to each part individually by assigning element size and mesh method. The meshed model is shown in Figure 4.2. Table 4.3 shows the mesh properties for each part of the generator.

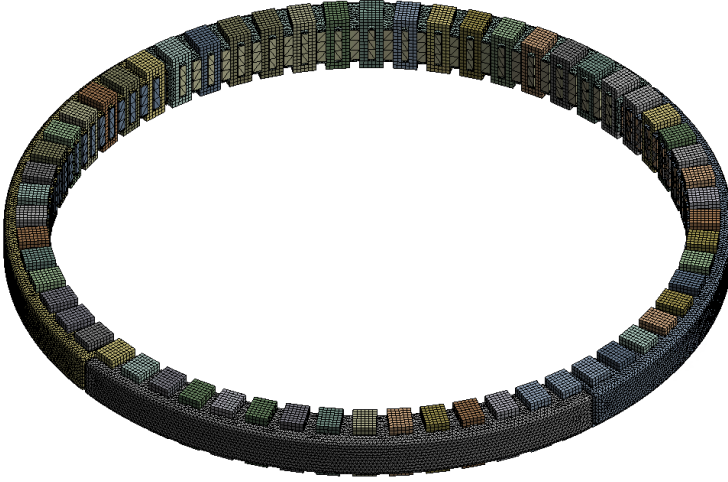


Figure 4.2: Meshing of segmented generator. Rotor and magnets are suppressed.

Table 4.3: Mesh properties of generator in ANSYS.

Part	Mesh	Element Type	Element Size
Coils	Sweep	Quad	0.01 m
Magnets	Sweep	Quad	0.01 m
Stator	Hex Dominant Method	Quad/Tri	0.05 m
Rotor	Tetrahedons	Tri	0.07 m
Insulation	Hex Dominant Method	Quad	0.01 m

4.2 NX

The models used for analyses in NX are shown Figure 4.3. One segment of the generator was analysed with different concepts of fastening. With the use of the Generator Configurator, two concepts of fastening can be activated. The first concept have an air-gap between the stator and stator ring. The second concept have an insulating layer between the stator and stator ring. Both concepts uses I-profiles of a composite material as fastening. The concepts and choice of materials are further explained in Magnus Borgersen's thesis.

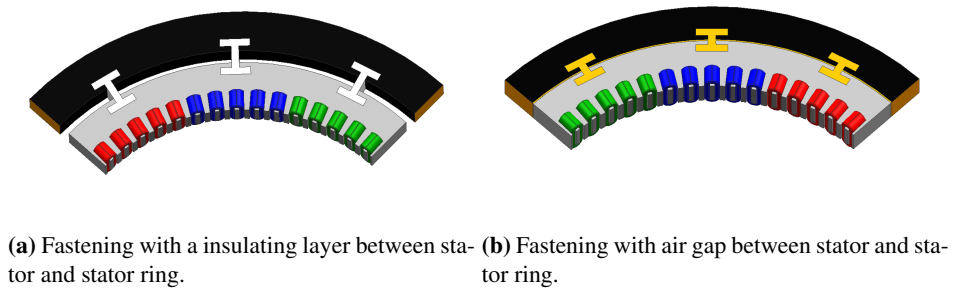


Figure 4.3: The two models used for thermal and coupled analyses in NX. Different concepts of fastening.

4.2.1 Materials

The materials are assigned in the `.fem` file in the pre/post application in NX. Assigned materials are listed in Table 4.4. The material of the fastening are decided to be a Nylon 66 glass fibre mix. All material properties can be seen in Table A.3 in Appendix A.

Table 4.4: Material assignment of the generator used in NX.

Part	Material
Coils	Copper C10100
Stator	Iron 40
Stator Ring	Steel
Fastening	Nylon Glass Fibre Mix

4.2.2 Mesh

The mesh is applied in the `.fem` file to the individual parts of the models, and is shown in Figure 4.4. Since the purpose of these analyses was to explore the thermal solvers in NX,

all parts were assigned a 3D Tetrahedral mesh with CTETRA(10) elements. The mesh properties are listed in Table 4.5.

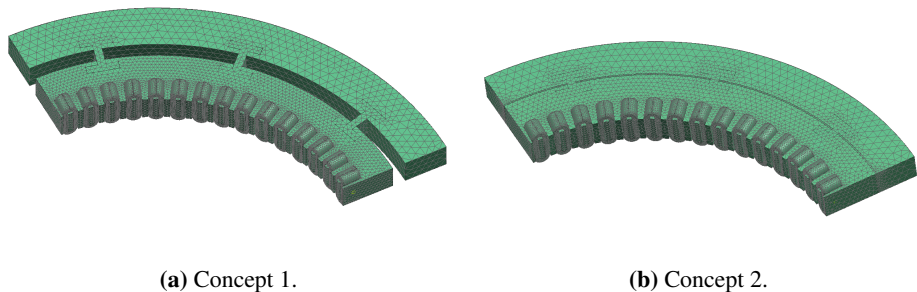


Figure 4.4: Meshing of the two generator segments.

Table 4.5: Mesh properties of generator in NX.

Part	Mesh	Element Type	Element Size
Coils	3D Tetrahedral	CTETRA(10)	10 mm
Stator	3D Tetrahedral	CTETRA(10)	10 mm
Stator Ring	3D Tetrahedral	CTETRA(10)	30 mm
Fastening	3D Tetrahedral	CTETRA(10)	15 mm

4.2.3 Mesh Mating

The tool *Mesh Mating - Free Coincident Condition* was used on the contacting surfaces. This creates a continuous mesh with aligned nodes between the different bodies. The contacting surfaces were selected automatically. Figure 4.5 shows the mesh mating applied to the two concepts.

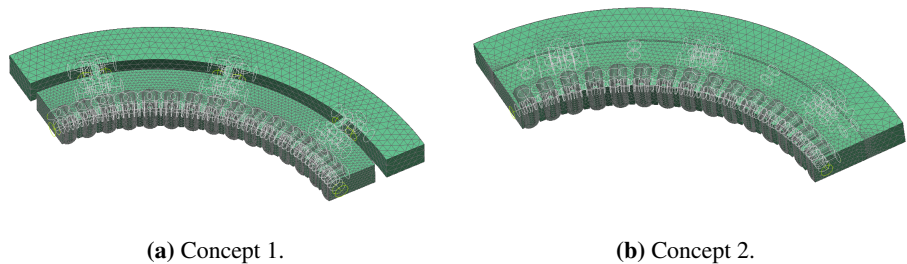


Figure 4.5: Mesh mating of the two models.

Chapter 5

Finite Element Analysis in ANSYS

5.1 Workflow



Figure 5.1: Overview of project approach.

An overview of the deployed tools in the project is illustrated in Figure 5.1. All the modelling and design of the generator were performed in Siemens NX and imported through ANSYS Workbench. The electromagnetic analyses were executed in ANSYS Maxwell. Thermal and mechanical analyses were performed in ANSYS Mechanical. Work related to digital twin monitoring were performed in ANSYS Twin Builder, with the key failure modes in focus. Geometry and analyses were coupled through ANSYS Workbench.

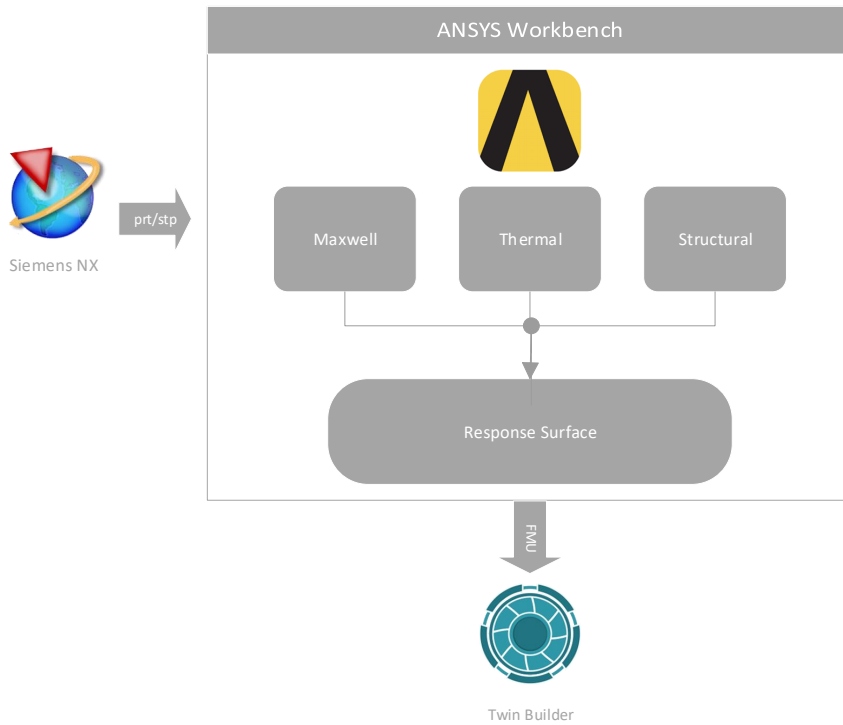


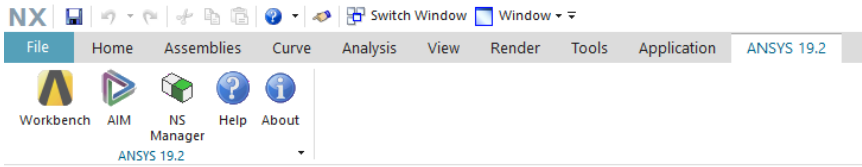
Figure 5.2: Workflow and communication between software.

The workflow of this project is illustrated in Figure 5.2. The Generator Configurator in Siemens NX was used to generate the geometry of the generator, while ANSYS Workbench was used as the interface for coupled analyses. The model was imported to ANSYS as a .prt or .stp file through the Geometry Interface in ANSYS Workbench. For use in the electromagnetic analyses in Maxwell 2D, it was necessary to import the geometry as a .stp file in order to create a 2D design. Thus, the link to NX was broken. For use in the thermal and structural analyses in ANSYS Mechanical, the geometry was imported as a .prt file through the Geometry Interface keeping the link between NX and ANSYS.

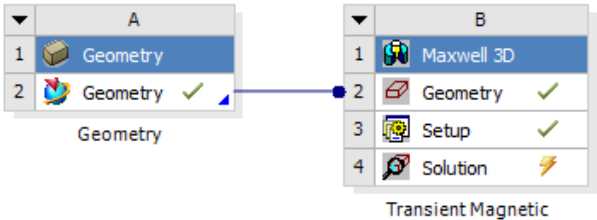
The results from the multi-physics simulations were used to create a Response Surface through ANSYS Workbench. Input and output parameters was selected in the respective software's. The response surface was exported as a FMU and implemented in ANSYS Twin Builder.

5.2 Coupling of NX and ANSYS

The geometry .prt file was directly imported using the integrated ANSYS Workbench interface in NX shown in Figure 5.3a, and integrated in ANSYS Workbench with the Geometry Interface as seen in Figure 5.3b. All geometry changes done in NX will then be reflected in the geometry in ANSYS Workbench. The ANSYS analysis domains used in this project are electromagnetic analysis in Maxwell 2D, steady-state thermal analysis, static structural analysis and modal analysis.



(a) The ANSYS Workbench Geometry Interface for NX.



(b) Importing the NX geometry in ANSYS Workbench, and using it in a transient electromagnetic analysis.

Figure 5.3: Integration of NX geometry into ANSYS Maxwell.

The parameters created with the Generator Configurator can be imported to ANSYS by using the prefix DS or ANS in the expressions created in NX. This permits performing analyses by easily changing the geometric configuration. The geometric parameters can be used as input when performing co-simulation.

to unexpected challenges, the electromagnetic analyses was performed the same way as in the project paper. To obtain a high accuracy in coupled electromagnetic and thermal analyses, the electromagnetic analysis should be performed in 3D on the same geometry as in the thermal analysis. To shorten the simulation time, the electromagnetic analysis was performed in 2D at this stage of the project. The 2D geometry was created by importing a .stp file of the NX geometry. The link to NX was thus broken for the electromagnetic analyses.

5.5 Thermal Analysis

5.5.1 Method

The thermal analyses were performed in ANSYS Mechanical with the interface Steady-State Thermal. Electromagnetic losses were computed in ANSYS Maxwell and imported into the steady-state thermal analysis as a thermal load. The resulting temperature can be exported to structural analyses in ANSYS Structural. The temperature can also be exported back to ANSYS Maxwell to account for temperature dependencies in material behaviour. The method is illustrated in Figure 5.5.

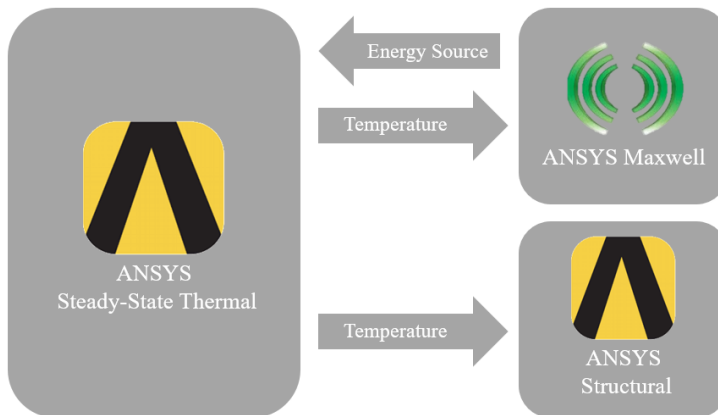


Figure 5.5: Overview of thermal analysis approach.

The coupling between the electromagnetic analyses and thermal analyses were done by dragging the solution from Maxwell 2D to the setup in Steady-State Thermal in ANSYS Workbench. This is illustrated in Figure 5.4.

5.5.2 Boundary Conditions

A summary of the applied boundary conditions in the thermal analyses can be seen in Table 5.1.

Table 5.1: Properties of the applied boundary conditions in ANSYS Mechanical.

Parameter	Value
Initial temperature	22 °C
Convection coefficient	6 W/(m ² °C)
Internal heat generation	Imported from ANSYS Maxwell

Constraints

Figure 5.6 shows the constraints applied to the model. Convection was defined on all external faces of the generator exposed to surrounding air. Initial temperature of the surroundings was defined as 22 °C. Convection was set to 6 W/(m² °C) as discussed in Section 2.5.1.

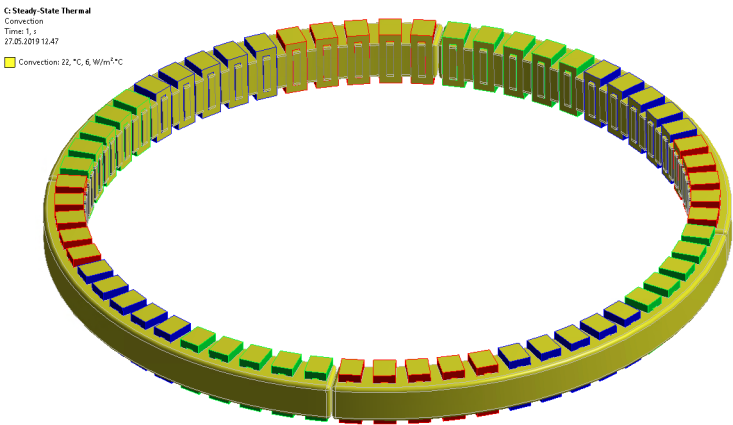


Figure 5.6: Convection defined on all external faces exposed to surrounding air.

Loads

Two load cases were simulated in ANSYS Steady-State Thermal. The first load case were imported from ANSYS Maxwell. Figure 5.7 shows the imported load in the solution of ANSYS Mechanical. The imported load occurs as a internal heat generation in the coils. Total loss can be seen in Imported Load Transfer Summary in Appendix C.4. Generated heat generation had a maximum of 68 200 W/m³ and the distribution can be seen in Figure 5.8a. The second load case was an evenly applied heat generation in the windings. As seen

in Figure 5.8b an internal heat generation with a magnitude of $60\,000\text{ W/m}^3$ was applied. By varying the convection coefficient on the four outer sides of the generator, the effect of heat transfer to the surroundings was explored. This was done to simulate cooling of the generator without the use of CFD analyses.

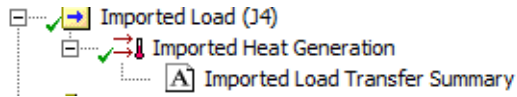
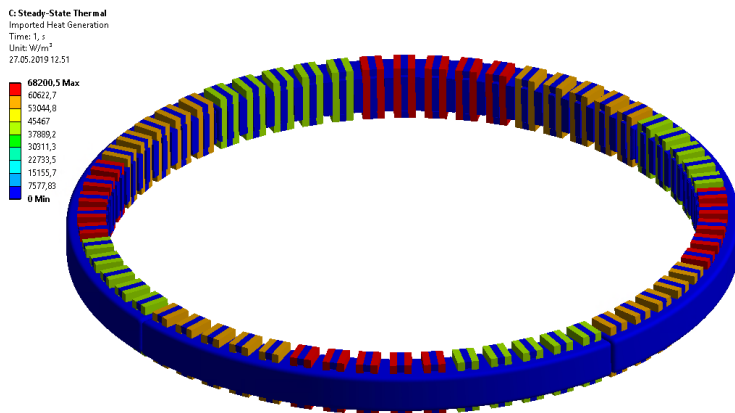
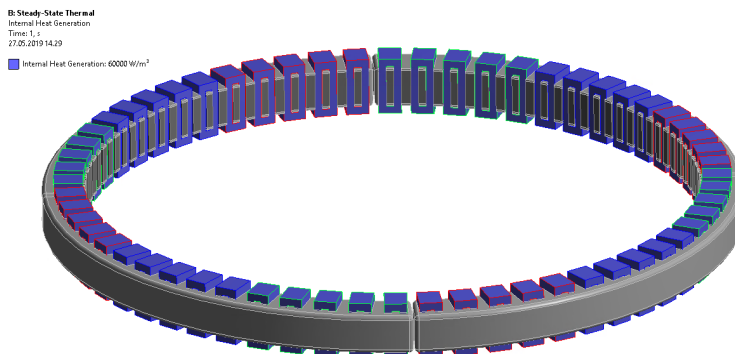


Figure 5.7: Imported load from ANSYS Maxwell.



(a) Heat generation imported from ANSYS Maxwell.



(b) Evenly applied internal heat generation in the windings.

Figure 5.8: The two load cases analysed in ANSYS Steady-State Thermal.

5.5.3 Simulation

The thermal analyses were performed using the Steady-State Thermal interface in ANSYS Workbench. This is a static solver and analyses is by default carried out in a single time step of 1 s. The default analysis settings were considered enough for the project at this stage.

5.6 Optimetric Analysis

5.6.1 Parameter Set

ANSYS has the ability to perform optimetric analyses by making a "sweep" of chosen input parameters. Parameters are defined in the individual software's and will be gathered in the Parameter Set in ANSYS Workbench. The parameter set are placed in the bottom of the Workbench setup, as seen in Figure 5.4. Figure 5.9 shows the parameter set in this project.

Outline of All Parameters				
	A	B	C	D
1	ID	Parameter Name	Value	Unit
2	☐ Input Parameters			
3	☐ Maxwell 2D Transient Segmented (D1)			
4	⚙ P5	velocity [rpm]	50	
*	⚙ New input parameter	New name	New expression	
6	☐ Output Parameters			
7	☐ Steady-State Thermal (C1)			
8	⚙ P6	Temperature Maximum	123,27	C
*	⚙ New output parameter		New expression	
10	Charts			

Figure 5.9: Parameters gathered in the Parameter Set in ANSYS Workbench.

5.6.2 Response Surface

Creating a response surface was done by using the Response Surface Interface in ANSYS Workbench, as seen in Figure 5.10. For creating a response surface, a set of input and output parameters needs to be created. When defining n parameters, a n -D response surface is created by doing a parameter sweep over all input parameters. The generator speed was set as the input parameter and the maximum temperature was set as the output parameter. First, the Design of Experiment was updated. By choosing the lower and upper bound for the generator speed, the design points were automatically created. The lower and upper bound were defined as 30 and 70, respectively. The five resulting design points can be seen in Figure 5.11.

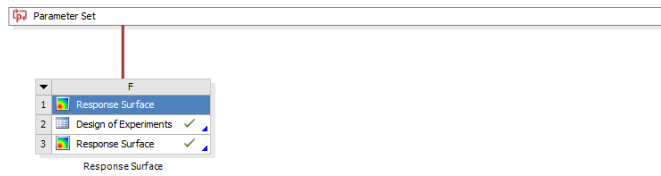


Figure 5.10: Response Surface interface in ANSYS Workbench.

	A	B
1	Name	P5 - velocity [rpm]
2	1 DP 0	50
3	2	30
4	3	70
5	4	40
6	5	60

Figure 5.11: Design points of Design of Experiment.

When a response surface is generated, it can be exported as a FMU (.fmu) or ROM (.dxrom) from the Response Surface Interface in ANSYS Workbench. The results were in this case exported as a FMU and further implemented in the ANSYS Twin Builder schematics.

Chapter 6

Thermal Analyses in NX Nastran

6.1 Thermal - SOL 153

As mentioned in Section 2.4, NX Nastran offers two solvers for thermal analyses: SOL 153 and SOL 159. The method for the SOL 153 solver will now be presented. As described, SOL 153 is a steady state heat transfer solver. It can be used for both linear and nonlinear problems. The models used in these analyses are shown in Section 4.2.

6.1.1 Boundary Conditions

The properties of the applied constraints and loads are gathered in Table 6.1.

Table 6.1: Properties of applied boundary conditions in NX.

Parameter	Value
Initial temperature	22 °C
Convection coefficient	6 W/(m ² °C)
Internal heat generation	60 000 W/m ³

Constraints

The thermal constraint that can be applied in this solver are, as mentioned earlier, temperature or convection. In this problem, free convection was applied to all external surfaces as shown in Figure 6.1. A heat transfer coefficient of 6 W/(m² °C) was defined as discussed in Section 2.5.1. Initial temperature of the surroundings was defined as 22 °C.

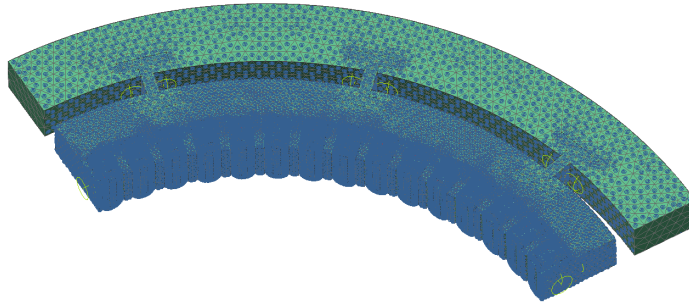


Figure 6.1: Convection defined on the model.

Loads

The thermal loads that can be applied are, as mentioned earlier, temperature, heat flux, radiation or heat generation. Here, an internal heat generation was applied to the coils in the model to simulate the electromagnetic losses that occur in a generator. The applied heat generation has a magnitude of $60\,000\text{ W/m}^3$ and can be seen in Figure 6.2.

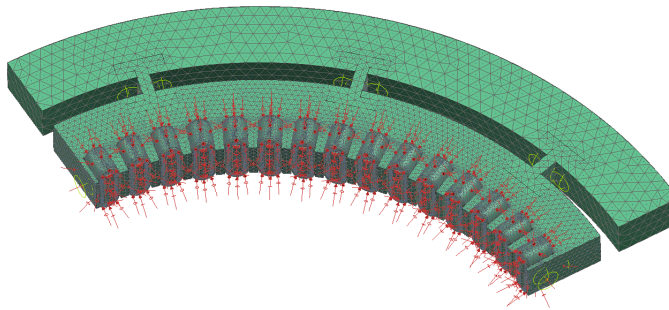


Figure 6.2: Internal heat generation applied to the model.

6.2 Coupled - SOL 101

By connecting the solution of the analyses performed in SOL 153 to a structural solver like SOL 101, one can perform coupled thermal and structural analyses. The temperature load is imported into the structural solution by creating a temperature set in the solution. First, an initial temperature was set to $22\text{ }^{\circ}\text{C}$ to create the temperature set as seen in Figure 6.3. Thereafter, a temperature load was created by importing the `.op2` result file from the thermal analyses in SOL 153 as seen in Figure 6.4.

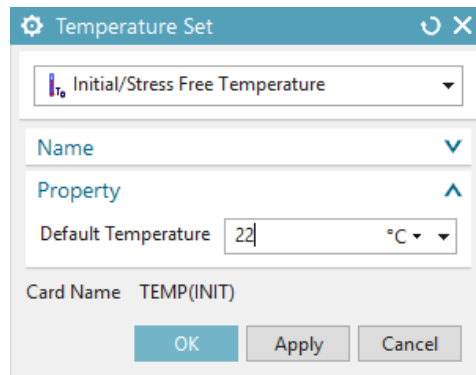


Figure 6.3: Initial temperature applied in a temperature set.

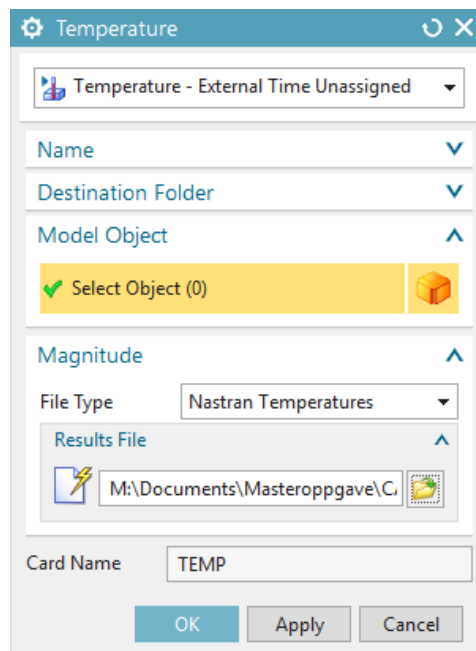


Figure 6.4: Temperature load imported to the temperature set.

The boundary conditions applied can be seen in Figure 6.5. Forces on the stator teeth (in red) was applied to simulate the radial forces common in electric machines. The ends of the stator support was constrained as fixed (in blue).

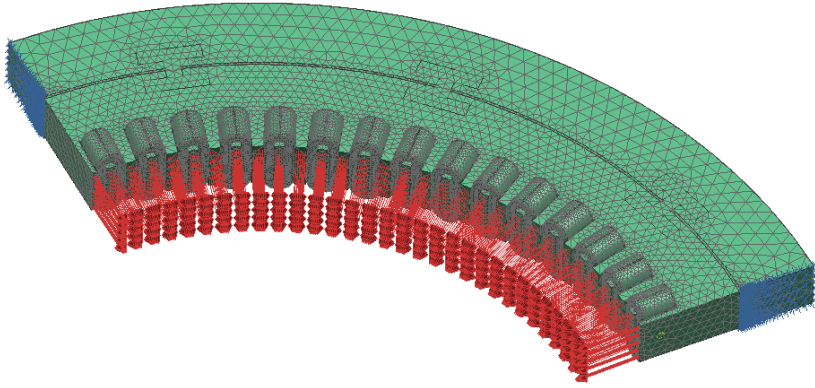


Figure 6.5: Boundary conditions in coupled thermal and structural analyses in NX.

Chapter 7

Thermal Benchmark

A thermal circuit was developed to benchmark the FEA results. The thermal circuit was created using the software *LTSpice*. To create a circuit equivalent to the thermal behaviour of a stator segment, the geometry in Figure 7.1 was used as reference. This is a section of a stator segment with one copper winding. The copper windings are insulated with a layer of thickness d_1 and the iron stator is insulated with a layer of thickness d_2 . The stator is surrounded by air on both sides with an inner temperature T_i and an outer temperature of T_y .

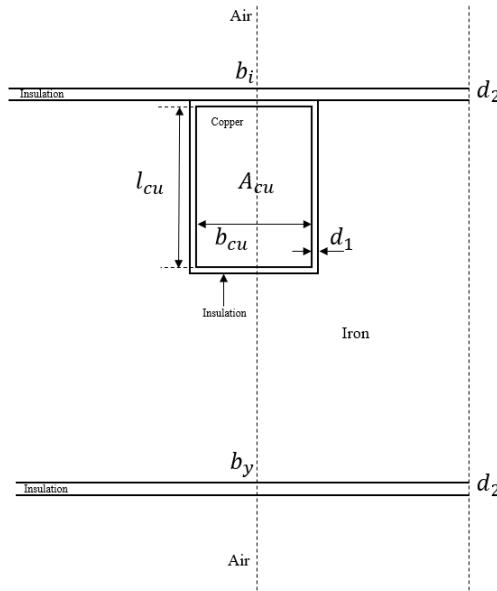


Figure 7.1: Geometry in equivalent thermal circuit.

The thermal circuit was created using the analogy defined in Table 2.3 in Section 2.5.2. Figure 7.2 shows the thermal resistance of each component. The thermal resistance of the iron was neglected in this model. I_1 is the heat generated in one half copper winding, R_1 is the thermal resistance of the top and bottom side of the copper insulation, R_2 is the thermal resistance of the right side of the copper insulation, R_i and R_y is the thermal resistance of the inner and outer side of the iron insulation, R_{oi} and R_{oy} is the thermal resistance of the heat transfer between the insulation and air on the inner and outer side.

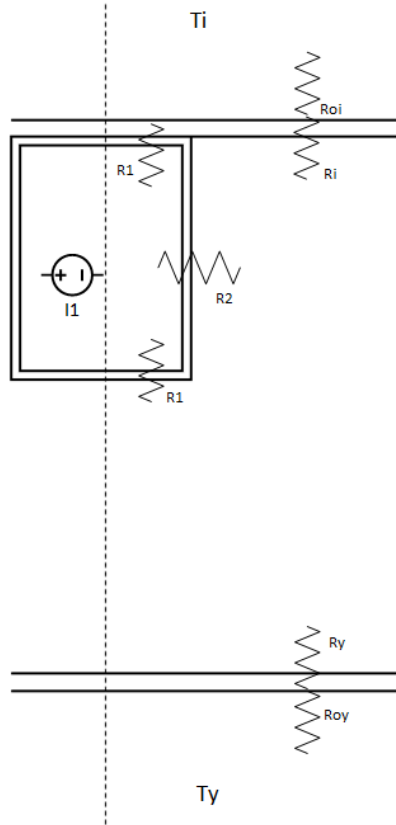


Figure 7.2: Thermal resistors of each component.

Equation 2.3-2.7 was used to calculate the thermal components in the circuit. The constants used in the calculations are listed in Table 7.1. Table 7.2 lists the resulting values of the thermal components. Results of the thermal circuit was used to benchmark the FEA thermal results. To recreate a similar load case in the FEA analyses, the heat generation was transformed to 3D. By dividing by the copper area of $\frac{1314}{2} \text{ mm}^2$, the resulting heat generation has a magnitude of $66\,971 \text{ W/m}^3$.

Table 7.1: Constants used in thermal circuit.

Constant	Value
J	2 A/mm^2
T_{air}	$22 \text{ }^\circ\text{C}$
h	$6 \text{ W/(m}^2 \text{ }^\circ\text{C)}$
d_1	1 mm
d_2	5 mm
δ_{el}	$5.96 \times 10^7 \text{ S/m}$
k_{iso}	0.3 W/(m K)
A_{cu}	1314 mm^2
b_{cu}	18 mm
l_{cu}	73 mm
b_i	82 mm
b_y	93 mm

Table 7.2: Resulting thermal components.

Component	Equation	Value
I_1	$J^2 \frac{A_{cu}}{\delta_{el}}$	44 W/m
R_1	$\frac{d_1}{k_{iso} \frac{1}{2} b_{cu}}$	0.37 m K/W
R_2	$\frac{d_1}{k_{iso} l_{cu}}$	0.05 m K/W
R_i	$\frac{d_2}{k_{iso} \frac{1}{2} b_i}$	0.41 m K/W
R_y	$\frac{d_1}{k_{iso} \frac{1}{2} b_y}$	0.36 m K/W
R_{oi}	$\frac{1}{h b_i}$	2.04 m K/W
R_{oy}	$\frac{1}{h b_y}$	1.79 m K/W

Chapter 8

Analysis Results

8.1 ANSYS

8.1.1 Steady-State Thermal

Temperature distribution resulting from load case 1, the coupled electromagnetic and thermal analysis, can be seen in Figure 8.1. The simulation time was approximately 2 minutes. Maximum temperature occurs in the windings in an even pattern that coincides with the applied load around the four segments and has a magnitude of 123 °C. Minimum temperature occurs on the outer surfaces of the iron stator and has a magnitude of 97 °C. The temperature on the inner stator teeth coincides with the winding temperature.

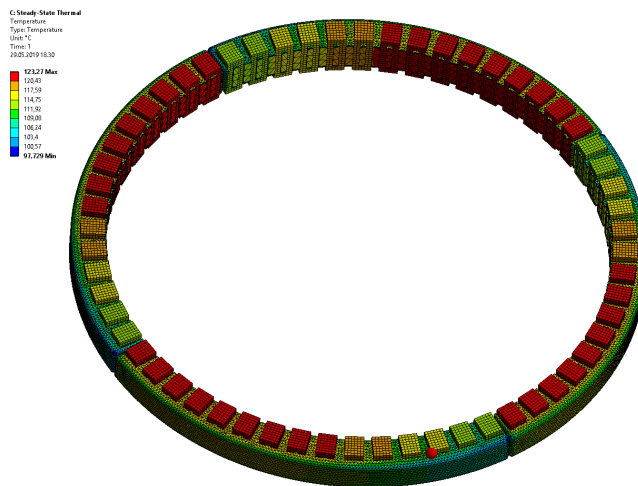


Figure 8.1: Temperature distribution from load case 1 - ANSYS Steady-State Thermal.

The resulting temperature distribution from load case 2, even internal heat generation in all windings, can be seen in Figure 8.2. The highest temperature occurs in the centre windings for each segment with a magnitude of 99 °C. The lowest temperature occurs on the outer surface of the stator at both ends of the segments with a magnitude of 79 °C.

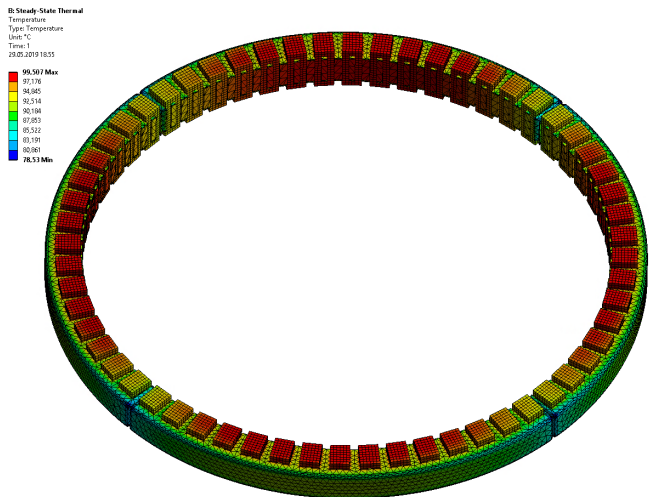


Figure 8.2: Temperature distribution from load case 2 - ANSYS Steady-State Thermal.

Table 8.1 shows the resulting minimum and maximum temperatures when increasing the convection coefficient on the outer generator faces. The maximum temperature occurs in the windings, while the minimum temperature occurs on the outer face of the stator segments. Figure 8.3 and 8.4 shows the relationships between the two temperatures and the convection coefficient. The parameter sweep showed that both maximum and minimum temperature decreases with an increasing convection coefficient on the outer faces. However, the maximum temperature eventually stabilises while the minimum temperature occurring in the iron stator has a steeper slope.

Table 8.1: Resulting temperature with varying convection coefficient.

Convection Coefficient	Temperature Max.	Temperature Min.
5 W/(m ² °C)	98.31°C	82.31°C
21.25 W/(m ² °C)	84.68°C	69.03°C
37.5 W/(m ² °C)	77.52°C	57.80°C
53.75 W/(m ² °C)	73.10°C	50.87°C
70 W/(m ² °C)	70.10°C	46.17°C

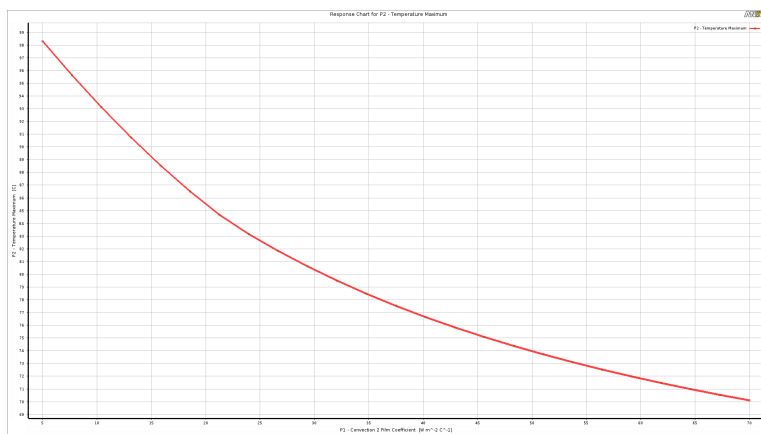


Figure 8.3: Maximum temperature in the windings over convection coefficient on outer faces.

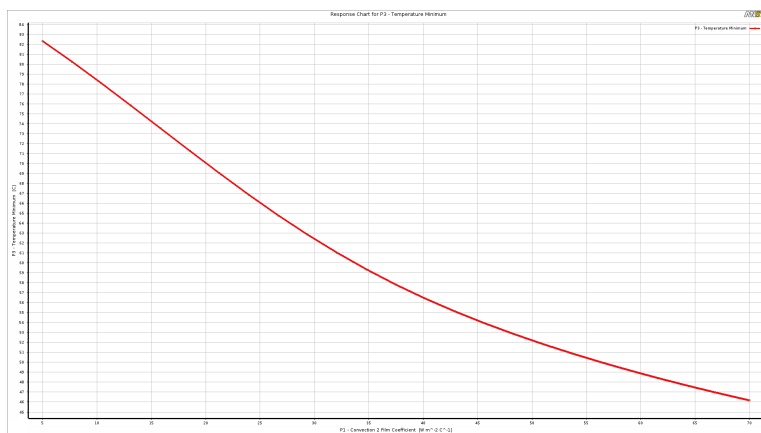


Figure 8.4: Minimum temperature in the windings over convection coefficient on outer faces.

8.1.2 Response Surface

The resulting design points from the update of Design of Experiment can be seen in Table 8.2. These were further used to generate the response surface seen in Figure 8.5. In this case only two parameters were used and the resulting response surface is thus a 2D response.

Table 8.2: Resulting design of experiment.

Generator Speed	Temperature Max.
30 rpm	124.77°C
40 rpm	124.31°C
50 rpm	123.27°C
60 rpm	123.46°C
70 rpm	123.36°C



Figure 8.5: Generated response surface showing temperature over velocity.

8.2 NX

This section will present the thermal and structural results from the analyses in NX. The purpose of these analyses was to explore the thermal solvers offered by NX Nastran, and the results will serve as a verification of realistic and reliable results.

8.2.1 SOL 153

The simulation time of the thermal analysis with SOL 153 was approximately 2 minutes. Figure 8.6 and 8.7 shows the resulting temperature in the two concepts using SOL 153. The highest temperature occurs in the windings with a magnitude of 75 °C for concept 1 and 94 °C for concept 2.

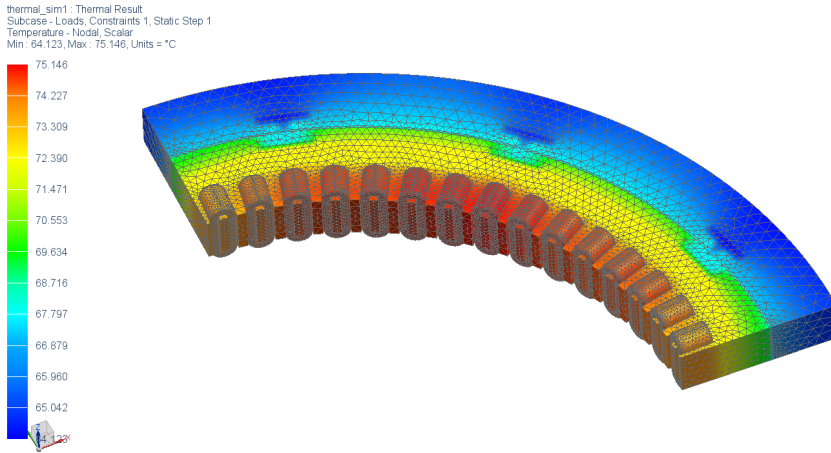


Figure 8.6: Temperature results on concept 1 - SOL 153.

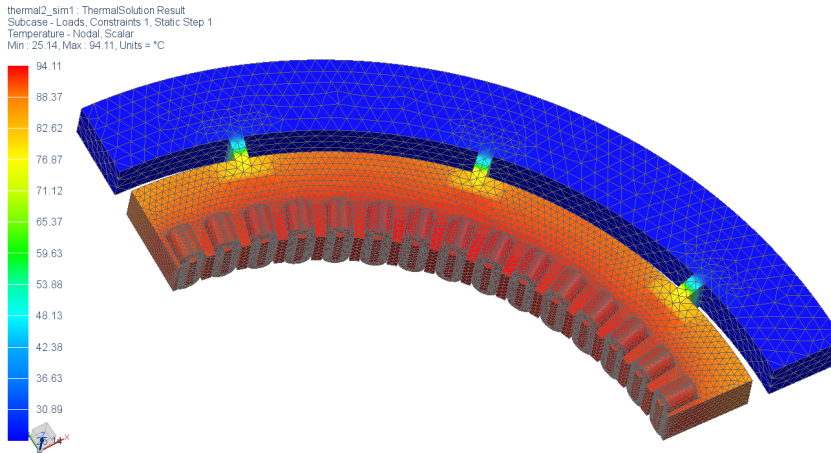


Figure 8.7: Temperature results on concept 2 - SOL 153.

8.2.2 SOL 101

The simulation time of the coupled structural and thermal analysis with SOL 101 was approximately 2 minutes. By doing coupled thermal and structural analysis one can retrieve thermal expansion, thermal stress and the effect of temperature in a certain load case. Figure 8.8 shows the resulting thermal expansion on concept 1 due to the thermal load applied. The highest deflection occurs at the top of the stator support.

SOL101(1)_sim1 : Solution 1 Result
 Subcase - Static Loads 1, Static Step 1
 Displacement - Nodal Magnitude
 Min : 0.000, Max : 0.793, Units = mm
 Deformation : Displacement - Nodal Magnitude

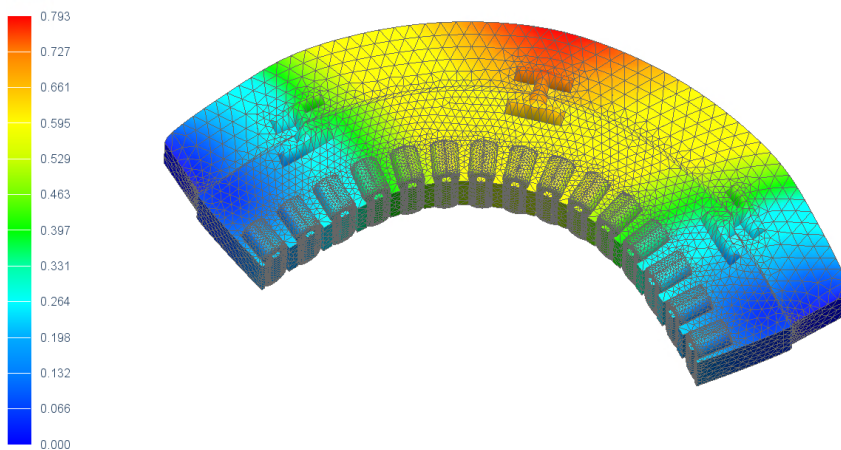


Figure 8.8: Displacement results on concept 1 - SOL 153/101.

8.3 Thermal Circuit

Figure 8.9 shows the resulting thermal circuit created using the software LTSpice. By running the circuit, the voltage values T_{cu} , T_{iron} , $T_{surface_i}$ and $T_{surface_y}$ was obtained. These values are equivalent to temperatures in the thermal circuit and have the unit of °C.

The resulting temperatures obtained from the thermal circuit can be seen in Table 8.3. Maximum temperature occurs in the copper windings and have a magnitude of 74 °C. The temperature in the iron stator are 72 °C, 2 °C below the copper temperature. Surface temperature on both the outer and inner side have a magnitude of approximately 64 °C. This will significantly depend on the convection coefficient between surface and surrounding air.

Table 8.3: Resulting temperatures from thermal circuit.

Component	Temperature
T_{cu}	74.11 °C
T_{iron}	72.38 °C
$T_{surface_i}$	63.93 °C
$T_{surface_y}$	63.95 °C

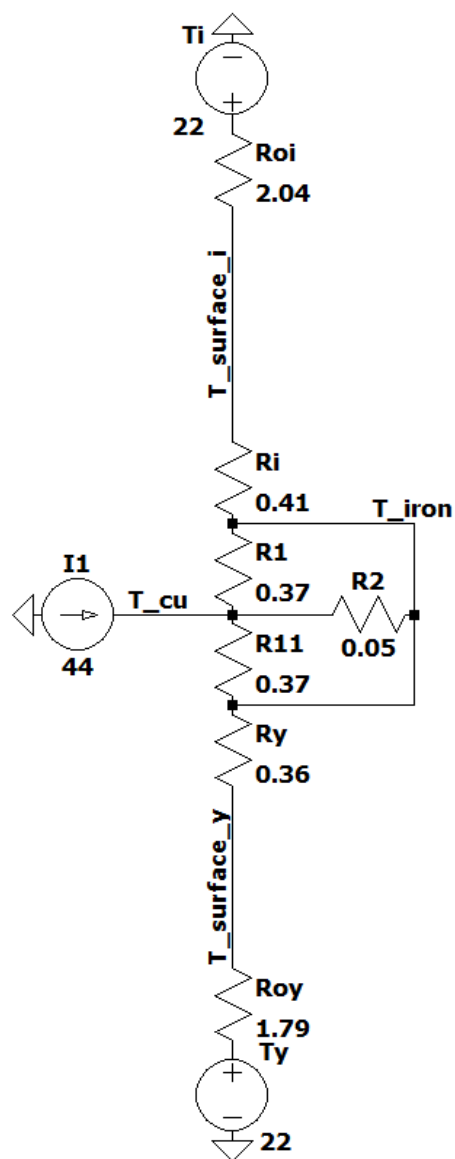


Figure 8.9: Resulting thermal circuit created in LTSpice.

Chapter 9

Digital Twin Solution

9.1 Digital Twin Applications of the ModHVDC Generator

As described in Section 2.6.2, the most common failure mode of electric machines is found to be bearing faults. This is often caused by too high temperatures and mechanical breakage due to vibration or poor lubrication. Summing up the parameters interesting to monitor, it is evident that the main faults to detect are high temperatures at specific locations and vibrations in the generator frame. Otherwise, monitoring of parameters like power and current of the generator are important. Thus this will be the parameters needed as an input to the digital twin model for it to be a useful implementation. Table 9.1 lists the resulting failure modes and how one can monitor them in the ModHVDC generator. Of the methods for condition monitoring previously described, performance, temperature, and vibration monitoring were found relevant for this project.

Table 9.1: The key parameters to monitor in a generator

Parameter	Possible fault mode(s)	Monitoring technique
Electrical parameters	High temperatures	Temperature sensors Monitoring power electronics
	Too high terminal voltage	
Stator and frame temperature	Insufficient cooling	Temperature sensors
Core and frame vibration	Interlaminar sliding Resonance vibration	Accelerometers on the frame
Rotor speed	Resonance vibration	Speed probe
	Mechanical fault in rotor	Accelerometers

9.1.1 Performance Monitoring

By monitoring parameters like current and output power one will receive information if the machine are in stable operation. If the sensor data indicates abnormal values, the digital twin can generate an alarm in the IIoT platform.

9.1.2 Temperature Monitoring

Monitoring of temperature is important as it is one of the common reason for failure in electric machines. Measurements of the temperature are crucial in digital twin monitoring and the temperature must lie within a certain limit to ensure stable operation. As seen in Chapter 8 maximum temperature occurs in the windings and thereafter the stator and stator insulation. Mounting of temperature sensors in the windings are difficult. Thus, virtual temperature sensor can be created as in the work described in Section 3.1 and 3.2. By creating a FMU with generator speed as input and maximum temperature as output, the temperature can be collected without any real sensors on the machine.

Sensors like thermocouples or thermistors are often used for temperature measurements in electric machines. Hence, bearings and coolant bulk outlet temperature can be monitored. An increase in bearing temperature can be an indication of incipient friction problems.

9.1.3 Vibration Monitoring

As previously stated, mechanical breakage can occur from damaged bearings, mechanical misalignment, abnormal rotor unbalance and eccentricity, shaft whirl and resonant torsional vibration. Structural vibration due to this mechanical breakage is of interest when preparing for monitoring with a digital twin.

Vibration monitoring is done by measuring parameters like displacement, velocity and acceleration. By placing accelerometers on a bearing blocks and stator segments, accelerations can be used as input in a FMU. The FMU can perform a FFT of this sensor data and show the frequencies of potential vibrations. Measurements of the machines rpm can be used as comparison with the FFT frequencies.

Bearing faults are a source of vibration and are best monitored by vibration, shock pulse and acoustic emission monitoring. It can be caused by improper lubrication and high stresses due to shaft deflection, inadequate mounting, alignment, or foundation. The results can be compared with measurements registered when the machine was new (or in a known condition). The sensitivity of this method is fairly high [12].

9.2 Framework for Digital Twin Monitoring

Architecture of a digital twin is illustrated in Figure 9.1 [18]. The physical asset is connected to a IIoT platform and provides data from the applied sensors. The IIoT platform is connected to cloud services and analyses the provided data. History of the asset is stored and alerts are triggered if the asset experience anomalies. The platform further provides the digital twin with the necessary input, and receives feedback from the simulation performed. This enables predictive maintenance and design feedback for the physical asset.

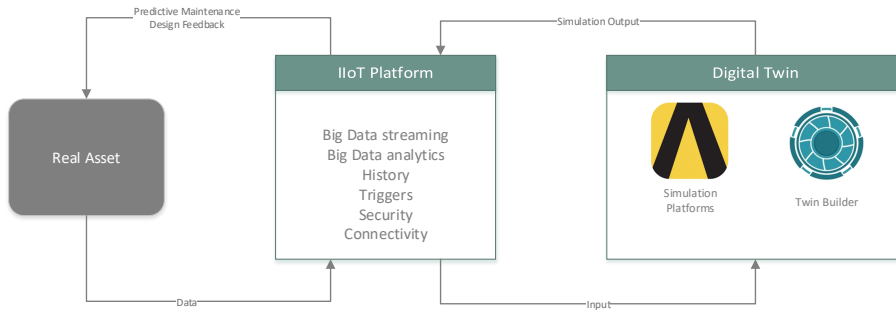


Figure 9.1: Digital Twin Architecture.

By studying the digital twin section of the architecture in Figure 9.1, a suggested framework for digital twin monitoring are created, as illustrated in Figure 9.2. It will receive input and provide simulation output to the IIoT platform. The digital twin framework consists of two FMUs for temperature and vibration monitoring. The vibration FMU is suggested to perform FFT on imported sensor data from accelerometers mounted on the generator. The vibration frequencies can then be monitored and compared to the rpm of the machine. Temperature can be monitored similar to the work described in Section 3, and function as a virtual temperature sensor.

Summarised, the most important parameters to implement, with or without the use of FMUs, in the framework for digital twin monitoring of the ModHVDC Generator are:

- Vibration
- Temperature
- RPM
- Current
- Power

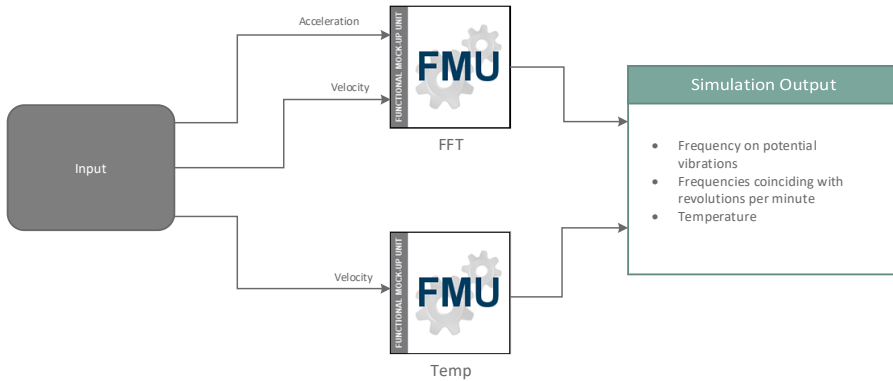


Figure 9.2: Framework for Digital Twin monitoring.

9.3 FMU Implementation

A FMU was created by exporting the response surface created in ANSYS Workbench. The FMU includes the electromagnetic analysis as well as the thermal analysis, and have generator speed as input and temperature as output. Figure 9.3 shows the implementation of the FMU in ANSYS Twin Builder schematics. Input was generated by using the component *Datapairs* where data sets with sensor data can be imported at a later stage. Since there exists no real sensor data in this case, input was simulated by creating an imaginary data set. The data set can be seen in Figure 9.4 and simulates a linear increase of generator speed from 25 rpm to 100 rpm.

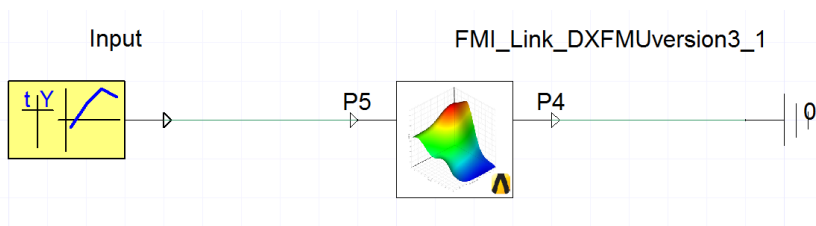


Figure 9.3: FMU implemented in ANSYS Twin Builder.

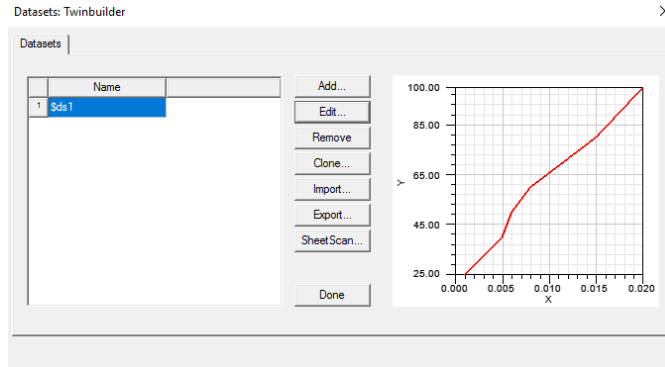


Figure 9.4: Data set implemented as input to the FMU.

By drawing a rectangular plot and tracing the input and output, one can monitor the temperature as a function of generator speed. The resulting trace for this FMU can be seen in Figure 9.5. The plot shows an increase of temperature up to approximately 53 rpm before dropping. At approximately 80 rpm the temperature stabilises.

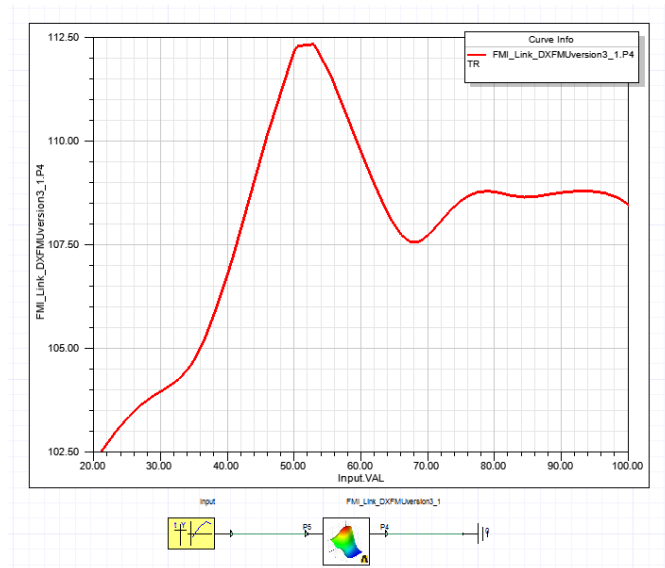


Figure 9.5: Resulting trace of temperature as a function of generator speed.

Chapter 10

Discussion

This chapter presents the discussion around the executed work. Challenges which occurred throughout the project are presented. It also aims to evaluate the obtained results and accuracy of the executed work. The sources of error are attempted identified.

10.1 Challenges

Various challenges and obstacles have occurred during the course of this project work. First, the project should have had more resources from the Department of Electric Power Engineering. When working on electric machines like the ModHVDC generator it becomes challenging when the majority of the project group have a mechanical engineering background. The lack of competence and understanding of basic concepts makes it difficult to contribute on the electromagnetic aspect of the project.

This thesis was dependent on getting the results of the electromagnetic analyses to perform coupled thermal analyses. Due to challenges along the way, the electromagnetic analyses performed by Marta Karoline Husebø from the Department of Electric Power Engineering required more time than initially planned. Lack of experience and limited resources within the use of ANSYS Maxwell made it difficult to obtain the needed results in time. Thus, the analyses have been more time-consuming than expected. To get started with the work, the electromagnetic analyses was therefore performed as the work done in the project report. When ready, the results from Marta Karoline Husebø's thesis can be included in this work.

10.2 Analyses

10.2.1 Simplifications

The approach of this project was to keep it as simple as possible in the beginning to ensure progress throughout the project period. This resulted in making simplifications both when creating the model of the generator, as well as in the analyses performed. The actual stator segments will consist of a laminated material which is neglected at this stage of the project. Initially the stator material is treated as isotropic which is expected to affect the accuracy of the analyses, both electromagnetic and thermal aspects. The copper windings are also treated as a solid body. They will in reality consist of insulated copper thread with an outer insulation layer. The outer insulation was attempted accounted for by calculating the total thermal conductivity in different directions. To reduce the simulation time, the copper windings were idealised by removing edge blends and other details. All this will affect the accuracy of the simulations, but was considered enough for the project at this stage.

10.2.2 Communication between NX and ANSYS

In an attempt to keep the geometry link between NX and ANSYS, as well as obtaining a better accuracy of the coupled analyses, it was decided to execute the electromagnetic analyses on a 3D system. However, 3D analyses requires significantly more computational time and a more advance setup. If every simulation in Maxwell requires 5 hours, parametric analyses needed to create a response surface would require a minimum of 25 hours. Thus, a 2D electromagnetic analysis was considered enough for the project at this stage. A 2D analysis in Maxwell introduces the issue of breaking the link between NX and ANSYS again. As Maxwell does not support conversion from a 3D system to 2D on a NX `.prt` assembly file, the 3D model must be exported as a `.stp` file from NX with the desired geometry. By doing this, all expressions and parameters from the geometry configurator are lost.

10.2.3 ANSYS

The resulting heat generation from the electromagnetic analyses in Maxwell coincides with the magnetic field in the generator. This is not an accurate scenario as the heat generation would be evenly distributed around the stator when the generator reaches steady-state. It was therefore chosen to execute thermal analyses with evenly applied heat generation in the windings. This resulted in a more realistic temperature distribution in the windings and stator. When the finished setup in ANSYS Maxwell performed by Marta Karoline Husebø is ready, it is expected to get a more realistic heat generation in the generator. Current results from the coupled analyses are therefore not considered as accurate due to the electromagnetic analyses.

The coupled analyses results in a maximum temperature of 123 °C and a minimum temperature of 97 °C. This is considered as high and will most likely lead to faults like insulation breakage. With evenly distributed heat generation, the maximum and minimum temperature are 99 °C and 79 °C. This is a more realistic result as copper temperatures can be expected to reach this range. When accounting for the lamination of the iron stator, lower temperatures are expected in the iron as this will result in lower thermal conductivity.

The convection coefficient is difficult to set with a high accuracy. It is often based on empirical values and will vary with the surroundings. In the analyses performed in this thesis, a value of 6 W/(m² °C) has been used. In air the convection coefficient usually lies in the range 5-12 W/(m² °C), and the chosen coefficient is thus in the lower section. The temperature can thus become significantly lower by choosing a slightly higher convection coefficient. By choosing a convection coefficient of 12 W/(m² °C), the maximum and minimum temperature becomes 59.8 °C and 56.9 °C.

As seen in Figure 8.3 and 8.4 both the maximum and minimum temperature are highly dependent on the convection on the outer face of the stator segments. This implicates that air cooling will have a significant effect on the temperatures in the generator. The temperature in the iron will have a steeper slope than the maximum temperature as this is more affected by the outer surface. The temperature in the copper will stabilise at a higher temperature as this is where the main losses occur. The effect of cooling should be further explored. However, this requires competence on CFD analyses. Varying the convection coefficient only gives an indication of the cooling effect.

10.2.4 NX

Analyses performed in NX was performed to study and test the thermal solvers SOL 153 and SOL 159. The results showed copper temperatures of 75 °C and 94 °C for the two stator fastening concepts. This implicates that the chosen fastening concept will have significant impact on the occurring temperature in the generator. The results matches the results obtained from similar analyses performed in ANSYS.

The load case in the performed coupled analysis is set up to simulate the electromagnetic forces in an electric machine. The forces will work in a sinusoidal pattern around the stator which coincides with the magnetic field. However, this is not based on the actual electromagnetic load case. It is therefore assumed that coupled analyses would achieve a higher accuracy when performed through ANSYS, with load cases directly from ANSYS Maxwell. For analyses in projects such as the ModHVDC project, it would therefore be beneficial to keep the analyses in ANSYS with the ability to perform direct coupled analyses.

10.2.5 Thermal Benchmark

When creating the thermal circuit, several simplifications were made. The resistance in the iron stator was neglected which is expected to lead to a lower temperature than in the FEA

analyses and reality. The resulting copper temperature from the thermal circuit is 74 °C. FEA analyses with evenly distributed heat generation lead to a maximum temperature of 99 °C, which is significantly higher than the temperature obtained from the circuit. This may be caused by oversimplification of the circuit, and implicates that the thermal resistance in the iron stator is an important factor. However, due to the simplifications of the circuit the FEA results are considered to be in a reasonable range. The thermal circuit will thus give a indication of the temperature range in the generator.

10.3 Digital Twin Monitoring

10.3.1 Failure Modes

Not as many failure modes of interest have occurred during the work done within digital twin monitoring as expected. Structural vibration due to eccentricity or bearings faults seems to be the parameter of most interest. Temperature is also an important parameter when monitoring an electric machine like the ModHVDC generator. When initialising the project, it was expected to find more relevant parameters for digital twin monitoring. This implicates that the ModHVDC generator might not be as suited for digital twin monitoring as initially assumed.

The project is still in an early face, and final design has not yet been determined. It was therefore concluded that making a prototype of the generator was too early at the current state of the project. However, this is possible within the next stages of the project work. When a prototype of the generator is created, real sensor data can be imported and implemented in ANSYS Twin Builder.

10.3.2 FMU Creation

Creation of FMUs is in this work performed by exporting response surfaces. This is a time-consuming process, and will require even more simulation time when the electromagnetic analyses are performed in 3D. It also provides low accuracy as it is interpolated from the response surface. To improve this in the future, the analyses should be exported to a FMU using the Static ROM Builder. This leads to a higher accuracy. Currently, this is only available for ANSYS Fluent.

The FMU implemented in Twin Builder schematics have generator speed as input and temperature as output. Initially, the aim was to include the output power of the generator as an input parameter in the FMU. However it was not found possible to choose this as a parameter in Maxwell.

As there is no sensor data to use as input in the FMU, a data set with a linear sweep of generator speed was imported. This is done to explore the implementation of FMUs in Twin Builder, not to obtain usable results. The trace shown in Figure 9.5 is not considered

a reliable results and the temperature response is expected to change when a more accurate FMU is created and real sensor data is used as input.

10.3.3 ANSYS Twin Builder

As ANSYS Twin Builder is a relatively new release, it is challenging to find documentation, applications and previous work of digital twin development using the software. Among the few published work are the GE wind turbine and PTC pump and electric motor system. It has been an work-some process to study the Twin Builder schematics and attempting to implement the created FMUs. With limited resources and lack of competence on the software, trial-and-error were necessary to achieve results.

ANSYS Twin Builder gives the impression of being premature, and still lacks some key features for creating digital twins. With the currently used version, ANSYS R19.2, export of the digital twins are still not available. In the previous work described, it is assumed that beta versions of the Twin Builder are used to create the digital twins. As mentioned, creation of FMUs with the use of the Static ROM Builder is not available to other domains than ANSYS Fluent.

Chapter 11

Conclusion and Further Work

11.1 Summary and Conclusions

The first objective of this thesis was to study the multidisciplinary ANSYS digital twin concept, Twin Builder. Literature and documentation of the software are presented in Section 2.3. Twin Builder are further used as the domain for the second objective, which is to implement a top-down framework for digital twin monitoring of the ModHVDC generator. The main failure modes to monitor were found to be high temperature and vibrations in the generator frame. Based on this, a digital twin monitoring framework has been suggested in Figure 9.2. A FMU monitoring the vibration frequencies and a FMU monitoring the temperature are implemented. As discussed in the Discussion, ANSYS Twin Builder gives the impression of being premature as it still lacks some key features. The ModHVDC project was also expected to lead to the discovery of more failure modes of the generator. This can be the results of the project being in an early phase.

The third objective was to establish a ROM, based on a response surface model, relating generator speed, output power and generator heat distribution similar to the work done on the GE Haliade Wind Turbine. A response surface was created from the coupled electromagnetic and thermal analyses. The input was defined as generator speed and output was defined as maximum temperature on the stator segments. Output power was not possible to define as an output from ANSYS Maxwell. The response surface model was exported as a FMU and implemented in the ANSYS Twin Builder schematics. Implementation of the FMU in Twin Builder schematics can be seen in Section 9.3. A FMU based on a response surface can be inaccurate as it is based on interpolation from the response. The FMU is thus implemented to explore the Twin Builder schematics and the results should not be considered reliable.

The fourth objective was to perform coupled analyses based on the performed electromagnetic analyses in ANSYS Maxwell. Unexpected challenges led to execution of the electromagnetic analyses based on the work done in the project report. The coupled ther-

mal analyses resulted in a maximum temperature of 123 °C and a minimum temperature of 97 °C. The temperature distribution coincided with the magnetic field from ANSYS Maxwell, which is considered inaccurate. By performing a thermal analysis with evenly distributed heat generation in the windings, maximum and minimum temperatures of 99 °C and 79 °C were obtained. This temperature distribution is even around the stator segments and is considered a more realistic distribution. The results are highly dependent on the applied convection coefficient, which was in the lower range in these analyses. The effect of cooling was attempted simulated, and both maximum and minimum temperature showed a significant decrease as the convection coefficient on the outer faces was increased, as seen in Figure 8.3 and 8.4.

The last objective was to study the NX Nastran thermal solvers. SOL 153 and SOL 159 were studied and tested by performing thermal and coupled analyses on two stator segments with different concept of stator fastening. The resulting maximum temperatures in the stator segments are 75 °C and 94 °C for concept 1 and 2 respectively. In projects like the ModHVDC project, it is concluded that direct coupled analyses in ANSYS is most beneficial.

At last, a thermal circuit of a stator segment is created to benchmark the thermal analyses performed in ANSYS and NX. The resulting copper temperature is 74 °C while the iron temperature is 72 °C. As several simplifications were made to the thermal circuit, FEA results of approximately 90 °C is considered reasonable.

11.2 Further Work

As the ModHVDC project is a work in progress, some key points for future work are pointed out below.

- Include 3D electromagnetic analyses to obtain necessary accuracy.
- Perform analyses of cooling of the generator. This requires competence on CFD analyses and is the next step in thermal analyses. It could also be performed by varying the convection coefficient of the different surfaces of the model.
- Creating a prototype of the generator. With testing and mounting of sensors on the generator, sensor data can be brought into ANSYS Twin Builder.
- Create a FMU capturing the vibration behaviour of the generator. By using sensor data from accelerometers, vibration frequencies can be obtained by performing FFT on the data. This could be compared with the frequency of the generator.
- Complete a Digital Twin simulation in the ANSYS Twin Builder capturing the most critical failure modes with real sensor data. When a digital twin of the generator is ready to be initialised, the framework could be implemented in an external cloud service and IIoT platform. Sensor data with real-time measurement of the generator is brought in as input to the FMUs and remote monitoring of the key parameters would create an exact representation of the real load case.

Bibliography

- [1] Pål Keim Olsen. ModHVDC Research Application. Technical report, NTNU et. al., October 2018.
- [2] REN21. Renewables 2016 Global Status Report. URL: "<https://apps.uqo.ca/LoginSigparb/LoginPourRessources.aspx?url=http://www.deslibris.ca/ID/10091391>", 2016 (accessed Dec 1, 2018). OCLC: 1010981965.
- [3] Stefan Boschert and Roland Rosen. Digital Twin—The Simulation Aspect. In Peter Hehenberger and David Bradley, editors, *Mechatronic Futures: Challenges and Solutions for Mechatronic Systems and their Designers*, pages 59–74. Springer International Publishing, Cham, 2016.
- [4] GE Digital. Digital Twin. URL: "<https://www.ge.com/digital/applications/digital-twin>", accessed Mars 11, 2019.
- [5] Bernard Dion. Digital Twin Workflow and Applications. URL: "<https://uwm.edu/csi/wp-content/uploads/sites/450/2018/04/ANSYS-Digital-Twin-Workflow-and-Applications-FINAL2.pdf>", April 4, 2018.
- [6] ANSYS. ANSYS Twin Builder. URL: "<https://www.ansys.com/products/systems/ansys-twin-builder>", accessed Mars 21, 2019.
- [7] ANSYS. Simulation Capabilities of ANSYS Twin Builder. URL: "<https://www.ansys.com/products/systems/ansys-twin-builder/twin-builder-capabilities>", accessed May 23, 2019.
- [8] P. Goncharov, I. Artamonov, and T. Khalitov. *Engineering Analysis With NX Advanced Simulation*. Lulu Press, Inc, December 2014. Google-Books-ID: 8FZc-CAAAQBAJ.
- [9] Siemens NX. NX Nastran 12: Advanced Nonlinear Theory and Modeling Guide. URL: "https://docs.plm.automation.siemens.com/data_services/resources/nxnastran/12/help/custom/en_US/advanced_nonlinear/advanced_nonlinear_tmg.pdf", 2017.

-
- [10] Frank P. Incropera and Frank P. Incropera, editors. *Fundamentals of heat and mass transfer*. John Wiley, Hoboken, NJ, 6th ed edition, 2007. OCLC: ocm62532755.
- [11] W. Jürges. The heat transfer at a flat wall (Der Wärmeübergang an einer ebenen Wand), Beihefte zum Gesundh. Ing, 1:19, 1924.
- [12] O. V. Thorsen and M. Dalva. Failure identification and analysis for high-voltage induction motors in the petrochemical industry. *IEEE Transactions on Industry Applications*, 35(4):810–818, July 1999.
- [13] Petr Kadanik. A brief survey of AC Drive Fault Diagnosis and Detection. *Prague*, pages 1–24, 1998.
- [14] Geoff Klemptner. *Handbook of large turbo-generator operation and maintenance*. IEEE Press series on power engineering. Hoboken, N.J. Wiley, Piscataway, N.J. IEEE Press, 2008.
- [15] W. T. Cochran, J. W. Cooley, D. L. Favon, H. D. Helms, R. A. Kaenel, W. W. Lang, G. C. Maling, D. E. Nelson, C. M. Rader, and P. D. Welch. What is the fast Fourier transform? *Proceedings of the IEEE*, 55(10):1664–1674, October 1967.
- [16] Ansysinc. Using ANSYS Twin Builder to Create a Digital Twin of GE’s Haliade™ 150-6mw Offshore Wind Turbine. URL: “https://www.youtube.com/watch?v=3Y11nF4_pKY”, accessed December 2, 2018.
- [17] GE Renewable Energy. Haliade 150-6mw Offshore Wind Turbine | GE Renewable Energy. URL: “<https://www.ge.com/renewableenergy/wind-energy/turbines/offshore-turbine-haliade>”, accessed December 2, 2018.
- [18] Chris MacDonald, Bernard Dion, and Mohammad Davoudabadi. Creating a Digital Twin for a Pump. URL: “<https://www.ansys.com/about-ansys/advantage-magazine/volume-xi-issue-1-2017/creating-a-digital-twin-for-a-pump>”, 2017 (accessed May 24, 2019).
- [19] Kara Gremillion. Digital Twin of a Multiple Physics Motor Pump System | ANSYS Blog. URL: “<https://www.ansys.com/blog/digital-twin-motor-pump-system>”, May 2017 (accessed May 26, 2019).
- [20] Oeystein Krøvel. *Design of Large Permanent Magnetized Synchronous Electric Machines: Low Speed, High Torque Machines - Generator for Direct Driven Wind Turbine- Motor for Rim Driven Thruster*. Norges teknisk-naturvitenskapelige universitet, Fakultet for informasjonsteknologi, matematikk og elektroteknikk, Institutt for elkraftteknikk, 2011.
- [21] M. Valavi, A. Nysveen, R. Nilssen, R. D. Lorenz, and T. Rølvåg. Influence of Pole and Slot Combinations on Magnetic Forces and Vibration in Low-Speed PM Wind Generators. *IEEE Transactions on Magnetics*, 50(5):1–11, May 2014.
-

Appendix

A

Material Properties

Table A.1: Material properties for electromagnetic analyses in ANSYS Maxwell.

	Copper	M400-50A	NdFe35	Steel 1008
Relative permeability	0.9999991	(See B-H curve)	1.0997785	(See B-H curve)
Bulk conductivity [S/m]	58e6	2e6	625e3	2e6
Magnetic coercivity	-	-	-890e3	-
Mass density [kg/m ³]	8933	7872	7400	7872
Young's modulus [GPa]	120	200	147	200
Poisson's ratio	0.38	0.25	0	0.25

Table A.2: Material properties for analyses in ANSYS.

	Copper Alloy	Gray Cast Iron	Insulation
Thermal Conductivity [W/(m K)]	401	52	0.3
Specific Heat, C_p [J/(kg K)]	385	447	-
Mass density [kg/m ³]	8300	7200	-
Young's modulus [GPa]	110	110	-
Poisson's ratio	0.34	0.28	-

Table A.3: Material properties for analyses in NX.

	Copper C10100	Iron 40	Nylon Glass Fibre
Thermal Conductivity [W/(m K)]	387	52	0.3
Specific Heat, C_p [J/(kg K)]	385	447	-
Mass density [kg/m ³]	8920	7192	1570
Young's modulus [GPa]	114	126.2	15.5
Poisson's ratio	0.31	0.25	0.384

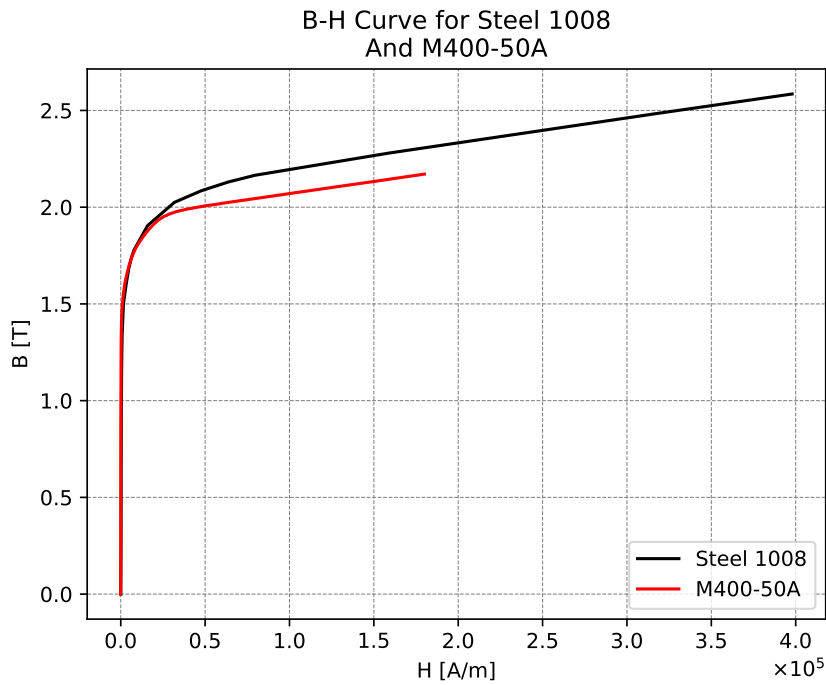


Figure A.1: B-H curve for Steel 1008 and M400-50A.

B

PM Generator Configurator

The Generator Configurator is created by Magnus Borgersen and is explained in further detail in his thesis. Figure B.2 and B.3 shows the menu used to create the model used in the analyses executed in this project. Figure B.1 shows an example configuration of the generator with 4 stator segments with fastening concept 1.

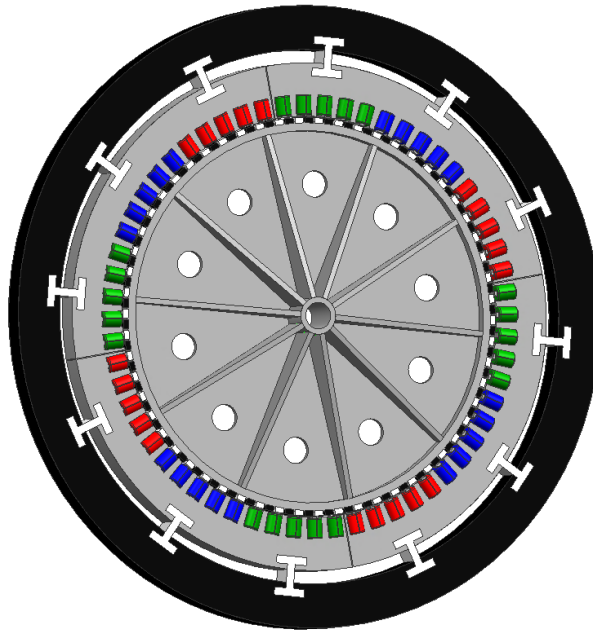
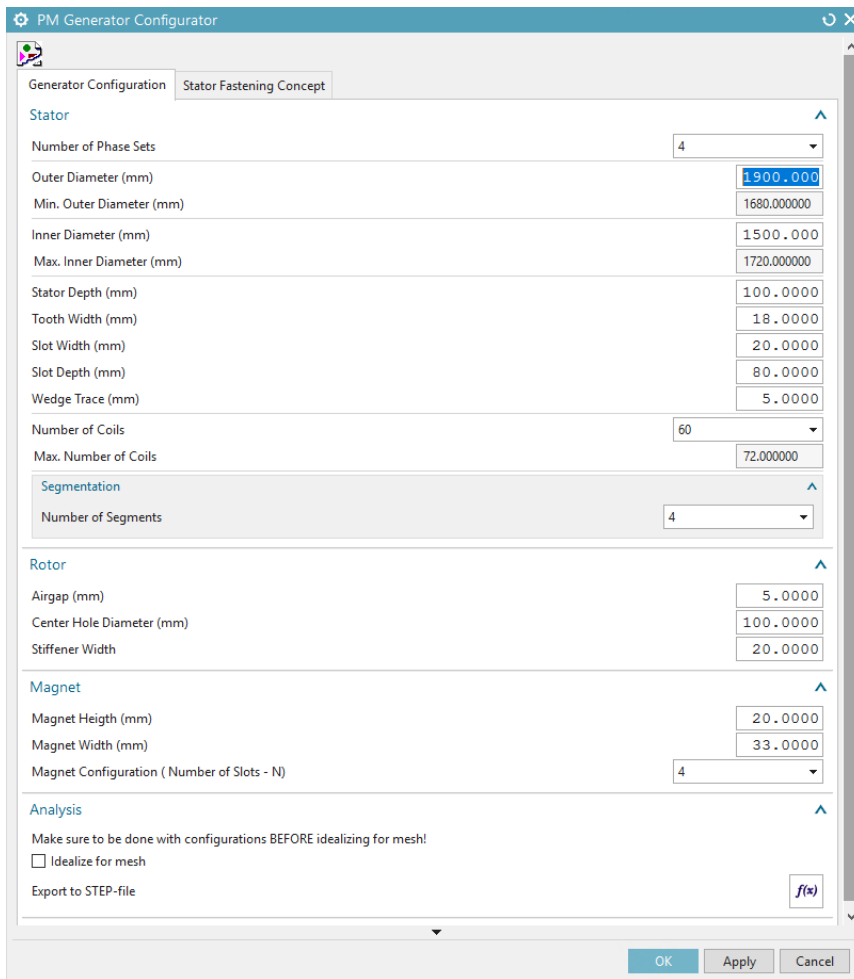


Figure B.1: PM Generator Configurator: Example configuration with stator fastening concept 1.



The image shows the 'PM Generator Configurator' window with the 'Generator Configuration' tab selected. The 'Stator Fastening Concept' sub-tab is also active. The 'Stator' section contains the following parameters:

- Number of Phase Sets: 4
- Outer Diameter (mm): 1900.000
- Min. Outer Diameter (mm): 1680.000000
- Inner Diameter (mm): 1500.000
- Max. Inner Diameter (mm): 1720.000000
- Stator Depth (mm): 100.0000
- Tooth Width (mm): 18.0000
- Slot Width (mm): 20.0000
- Slot Depth (mm): 80.0000
- Wedge Trace (mm): 5.0000
- Number of Coils: 60
- Max. Number of Coils: 72.000000

The 'Segmentation' section contains:

- Number of Segments: 4

The 'Rotor' section contains:

- Airgap (mm): 5.0000
- Center Hole Diameter (mm): 100.0000
- Stiffener Width: 20.0000

The 'Magnet' section contains:

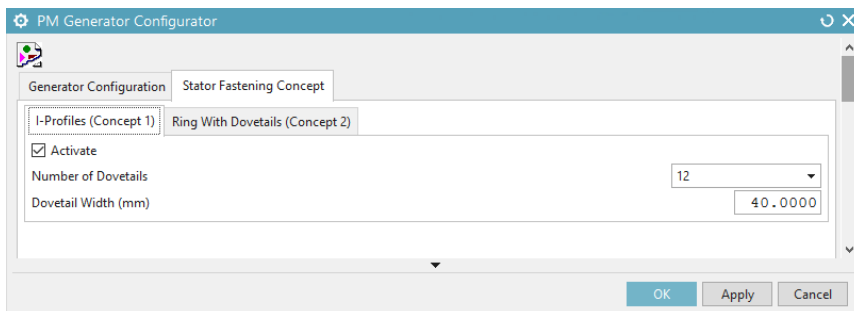
- Magnet Height (mm): 20.0000
- Magnet Width (mm): 33.0000
- Magnet Configuration (Number of Slots - N): 4

The 'Analysis' section contains:

- Make sure to be done with configurations BEFORE idealizing for mesh!
- ☐ Idealize for mesh
- Export to STEP-file f(x)

At the bottom, there are 'OK', 'Apply', and 'Cancel' buttons.

Figure B.2: PM Generator Configurator: Generator Configuration.



The image shows the 'PM Generator Configurator' window with the 'Generator Configuration' tab selected. The 'Stator Fastening Concept' sub-tab is active. The 'I-Profiles (Concept 1)' section contains the following parameters:

- ☒ Activate
- Number of Dovetails: 12
- Dovetail Width (mm): 40.0000

The 'Ring With Dovetails (Concept 2)' section is also visible but empty.

At the bottom, there are 'OK', 'Apply', and 'Cancel' buttons.

Figure B.3: PM Generator Configurator: Stator Fastening Concept.

C

Electromagnetic Analysis in ANSYS Maxwell

This chapter is taken from the project report written in the fall of 2018. It is reintroduced as this analysis is used as reference when performing the electromagnetic analyses in this thesis.

C.1 Requirements

Machine data of the generator used in throughout this project are listed in Table C.1. These parameters are the same as for the prototype generator in [20, 21]. This is done to compare the results of the segmented generator with a conventional machine.

Table C.1: Machine data of the prototype generator

Rated power	50kW	Number of coils	60
Number of phases	3	Number of turns	19
Rated frequency	50Hz	Stator stack length	100mm
Rated speed	51.7rpm	Stator slot depth	80mm
Current	120 A	Stator slot width	22.3mm
Electric Loading	56 kA/m	Stator inner diameter	1557mm
Number of poles	116	Stator outer diameter	1777mm
Number of stator slots	120	Air-gap length	5mm
Ampere Turn	2.3 kA	Magnet length	20mm
Remanent flux density	1.2 T	Magnet width	33mm
Stator material	M400-50A	Permanent magnets	NdFeB N35

C.2 Finite Element Analysis

The analyses are performed on a 2D cross section of the generator model, as seen in Figure C.1. The extraction of the 2D section makes it impossible to import the `.prt` file directly from NX. In order to overcome this, the model is imported as a `.stp` file. This breaks the link between NX and ANSYS. The solution type is chosen as a magnetic transient solution which computes the time-domain magnetic fields and losses. Setup in ANSYS Maxwell is done as in the project report.

Defining Motion in the Model

In order to define rotational motion to the rotor, the objects that are going to rotate must be isolated from the rest of the model. This is done by defining a mesh band, which is an user-defined geometry that contains all rotating parts. All parts contained in the mesh band will then move together as one rigid body. For the generator, the mesh band consists of a cylinder lying in the middle of the air gap between rotor and stator. When motion is applied, the stator will remain stationary while the rotor and magnets rotate at the set angular velocity. The angular velocity is defined as a variable and later set as an input when creating a FMU to be implemented in Twin Builder. This allows the rotational speed to be controlled externally, eventually from a sensor on the actual generator.

Assigning Materials to the Model

When the cross section of the model is imported into Maxwell 2D, all parts are defined as *Sheets*. Each sheet needs to be assigned a material, which can either be picked from a library of materials or a user defined material. For the magnets, the standard magnetic material NdFe35 is chosen, modified to have alternating polarity for north and south magnets. The coils are defined as traditional copper, and the rotor is defined as the standard material iron. As the stator is made out of laminates, the steel M400-50A was used, because it models the laminated steel's magnetic behaviour through its custom B-H curve. All material properties used in FE analyses are presented in Table A.1 and the B-H curve of steel M400-50A can be seen in Figure A.1.

Assigning Boundaries and Excitations

The outer boundary used for the generator is the *Balloon* type boundary. This boundary models the case where the structure is “infinitely” far away from other magnetic fields, permanent magnets, or current sources. It is used to model magnetically isolated structures. Two types of excitations are used in the model, coils and windings. The coils are assigned to a sheet, and the number of conductors and polarity of the coil is defined by the user. After assigning coils to all of the sheets representing the coils of the generator, three windings are added, one for each phase. Stranded windings with a resistance of 150m Ω and 4.7mH were defined. These parameters are taken from the electrical parameters found

for the prototype generator in [20]. The windings can be set as external, allowing the parameters of the windings to be controlled externally through Twin Builder. The winding layout can be seen in the Appendix, Figure C.2.

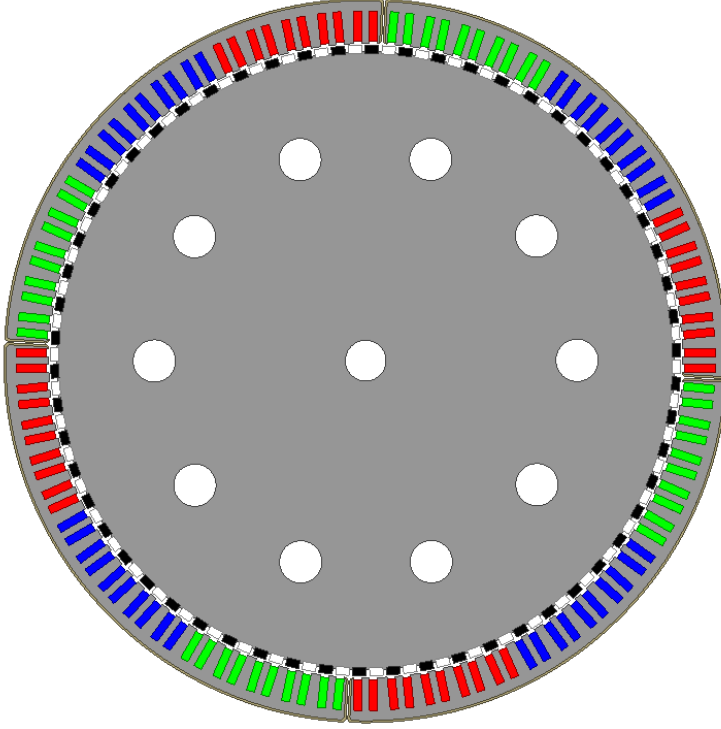


Figure C.1: 2D section of the generator used in analyses performed in ANSYS Maxwell.

C.3 Winding Layout

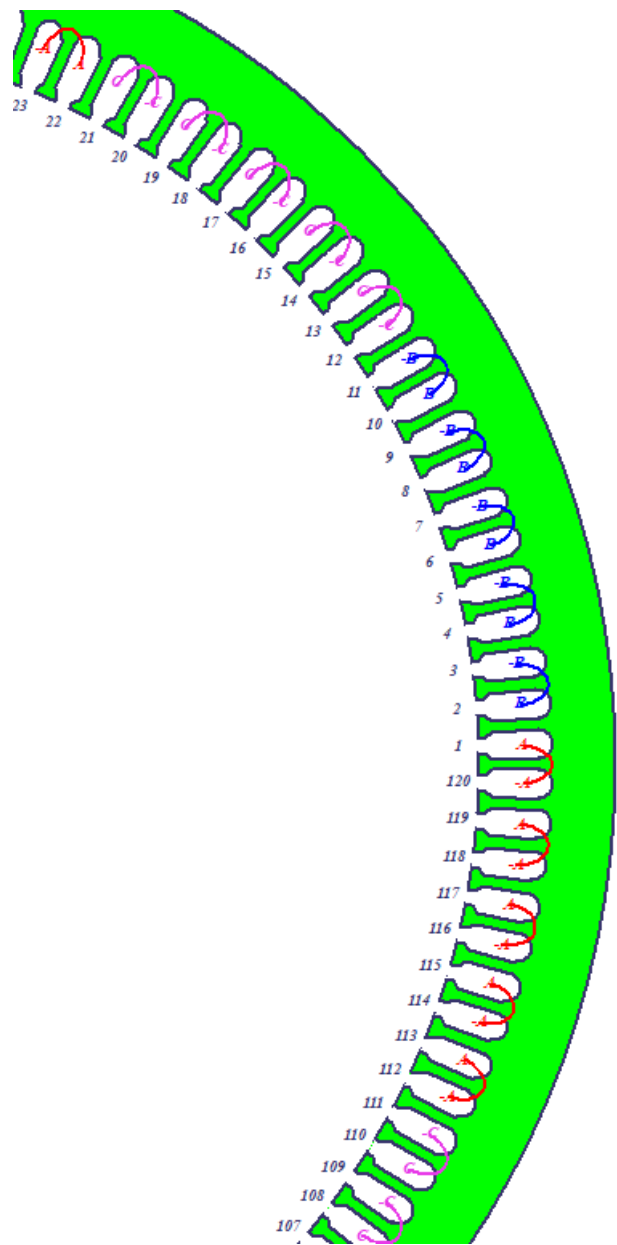


Figure C.2: Winding layout for the analysed generator.

C.4 Heat Generation from ANSYS Maxwell

The resulting heat losses from the analyses in ANSYS Maxwell are seen in Table C.2 below. This is imported as a thermal load in the thermal analyses in ANSYS Mechanical.

Table C.2: Imported Load Transfer Summary.

Object	Total Loss	Scaling Factor
Insulation Body 1	0W	0
Insulation Body 2	0W	0
Insulation Body 3	0W	0
Insulation Body 4	0W	0
Stator Body 1	0W	0
Stator Body 2	0W	0
Stator Body 3	0W	0
Stator Body 4	0W	0
coil_blue.C_1	15.074W	1
coil_blue.D	15.0723W	1
coil_blue.A_2	15.0723W	1
coil_blue.B_2	15.0552W	1
coil_blue.C_2	15.0552W	1
coil_blue.D_1	15.074W	1
coil_blue.D_2	15.0552W	1
coil_blue.A_3	15.0723W	1
coil_blue.B_3	15.0552W	1
coil_blue.C_3	15.0723W	1
coil_blue.D_3	15.0552W	1
coil_blue.A_4	15.0552W	1
coil_blue.B_4	15.0552W	1
coil_blue.C_4	15.0723W	1
coil_blue.D_4	15.0723W	1
coil_blue.B_1	15.074W	1
coil_blue.A	15.0723W	1
coil_blue.B	15.0552W	1
coil_blue.C	15.0552W	1
coil_blue.A_1	15.0723W	1
coil_green.D	8.58336W	1
coil_green.A	8.58336W	1
coil_green.B	8.58336W	1
coil_green.C	8.58336W	1
coil_green.D_1	8.57365W	1
coil_green.B_1	8.58433W	1
coil_green.A_1	8.58336W	1
coil_green.B_2	8.57365W	1

Continued on next page

Table C.2 – continued from previous page

First column	Second column	Third column
coil_green_C_1	8.58336W	1
coil_green_A_2	8.58336W	1
coil_green_D_2	8.58336W	1
coil_green_A_3	8.58336W	1
coil_green_B_3	8.57365W	1
coil_green_C_2	8.57365W	1
coil_green_D_3	8.58433W	1
coil_green_C_3	8.58433W	1
coil_green_D_4	8.57365W	1
coil_green_A_4	8.58336W	1
coil_green_B_4	8.57365W	1
coil_green_C_4	8.58336W	1
coil_red_D_4	11.9846W	1
coil_red_A_4	11.971W	1
coil_red_B_4	11.9846W	1
coil_red_C_4	11.9859W	1
coil_red_C	11.9846W	1
coil_red_D	11.9846W	1
coil_red_A	11.971W	1
coil_red_B	11.971W	1
coil_red_C_1	11.971W	1
coil_red_D_1	11.9846W	1
coil_red_A_1	11.971W	1
coil_red_B_1	11.9846W	1
coil_red_C_2	11.9846W	1
coil_red_D_2	11.971W	1
coil_red_A_2	11.9859W	1
coil_red_B_2	11.9859W	1
coil_red_A_3	11.9846W	1
coil_red_B_3	11.9846W	1
coil_red_C_3	11.9846W	1
coil_red_D_3	11.9846W	1
coil_blue_A_Separate1	15.0483W	1
coil_blue_A_1_Separate1	15.0552W	1
coil_blue_A_2_Separate1	15.0552W	1
coil_blue_A_3_Separate1	15.0483W	1
coil_blue_A_4_Separate1	15.0653W	1
coil_blue_B_Separate1	15.0658W	1
coil_blue_B_1_Separate1	15.0653W	1
coil_blue_B_2_Separate1	15.0653W	1
coil_blue_B_3_Separate1	15.0658W	1
coil_blue_B_4_Separate1	15.0658W	1
Continued on next page		

Table C.2 – continued from previous page

First column	Second column	Third column
coil_blue_C.Separate1	15.0658W	1
coil_blue_C_1.Separate1	15.0653W	1
coil_blue_C_2.Separate1	15.0653W	1
coil_blue_C_3.Separate1	15.0552W	1
coil_blue_C_4.Separate1	15.0552W	1
coil_blue_D.Separate1	15.0552W	1
coil_blue_D_1.Separate1	15.0653W	1
coil_blue_D_2.Separate1	15.0658W	1
coil_blue_D_3.Separate1	15.0653W	1
coil_blue_D_4.Separate1	15.0552W	1
coil_green_A.Separate1	8.57365W	1
coil_green_A_1.Separate1	8.57365W	1
coil_green_A_2.Separate1	8.57365W	1
coil_green_A_3.Separate1	8.57365W	1
coil_green_A_4.Separate1	8.57365W	1
coil_green_B.Separate1	8.57365W	1
coil_green_B_1.Separate1	8.57937W	1
coil_green_B_2.Separate1	8.57968W	1
coil_green_B_3.Separate1	8.57968W	1
coil_green_B_4.Separate1	8.57968W	1
coil_green_C.Separate1	8.57365W	1
coil_green_C_1.Separate1	8.57365W	1
coil_green_C_2.Separate1	8.57968W	1
coil_green_C_3.Separate1	8.57937W	1
coil_green_C_4.Separate1	8.57365W	1
coil_green_D.Separate1	8.57365W	1
coil_green_D_1.Separate1	8.57968W	1
coil_green_D_2.Separate1	8.57365W	1
coil_green_D_3.Separate1	8.57937W	1
coil_green_D_4.Separate1	8.57968W	1
coil_red_A.Separate1	11.9794W	1
coil_red_A_1.Separate1	11.9794W	1
coil_red_A_2.Separate1	11.979W	1
coil_red_A_3.Separate1	11.971W	1
coil_red_A_4.Separate1	11.9794W	1
coil_red_B.Separate1	11.979W	1
coil_red_B_1.Separate1	11.971W	1
coil_red_B_2.Separate1	11.979W	1
coil_red_B_3.Separate1	11.971W	1
coil_red_B_4.Separate1	11.971W	1
coil_red_C.Separate1	11.971W	1
coil_red_C_1.Separate1	11.9794W	1
Continued on next page		

Table C.2 – continued from previous page

First column	Second column	Third column
coil_red_C_2_Separate1	11.971W	1
coil_red_C_3_Separate1	11.971W	1
coil_red_C_4_Separate1	11.979W	1
coil_red_D_Separate1	11.971W	1
coil_red_D_1_Separate1	11.971W	1
coil_red_D_2_Separate1	11.979W	1
coil_red_D_3_Separate1	11.971W	1
coil_red_D_4_Separate1	11.971W	1

D

Modal Analysis

Modal analyses were performed on a single stator segment with stator fastening concept 1, as seen in Figure D.1. A fixed support was assigned to the outer face of the fastening ring in order to obtain only the modes of the stator segments. The resulting first 20 modal frequencies are listed in Table D.1.

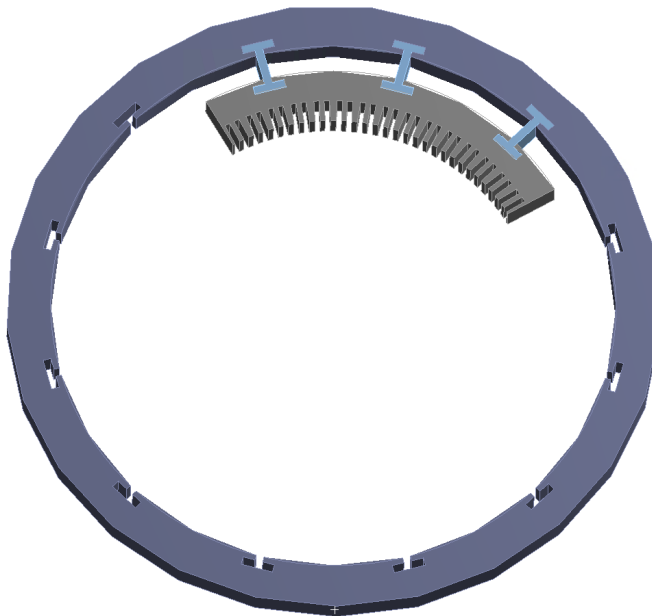


Figure D.1: Generator model used in modal analyses.

Table D.1: Resulting modal frequencies.

Mode	Frequency [Hz]
1	85.675
2	134.69
3	149.28
4	234.45
5	333.12
6	363
7	379
8	460.96
9	513.01
10	520.69
11	689.25
12	892.78
13	938.87
14	1061.2
15	1111
16	1133.3
17	1301.5
18	1336.7
19	1337.5
30	1379